Peer Review File

Manuscript Title: Self-regulated non-reciprocal motions in single-material microstructures

Note: The published paper has been further edited to comply with the journal's guidelines, and therefore the quotes in the response letter and the final manuscript are not identical.

Reviewer Comments & Author Rebuttals

Reviewer Reports on the Initial Version:

Referees' comments:

Referee #1 (Remarks to the Author):

The authors of the article have demonstrated an interesting self-regulated system using liquid crystal elastomer microposts. The misalignment among the axial direction of the micropost, liquid crystal orientation and the light direction leads to self-regulated motion of the system. Collective motion of multiple microposts have also been investigated. The authors have also conducted numerical simulations of the dynamic behaviors of the system, and the simulation results can quantitatively capture the complex behaviors of the system. It is a very nice piece of work and the studies done by the authors are careful and systematic. However, I fail to find an extremely strong point that make the presented work truly outstanding. Detailed comments are given below:

Many self-oscillation modes have been demonstrated in the literature and many of the previous examples are indeed based on light responsive LCEs with the associated mechanism as opto-chemo-mechanical coupling. I understand that the specific self-oscillation modes in the paper are different from previous studies. However, the major novelty of the study is not very clear to me. In another word, what really makes the paper outstanding? The authors claim the opto-chemo-mechanical feedback is unique. But, in my opinion, the mechanism is not really too different from the self-oscillation caused by the self-shadowing effects widely explored in the literature. For example, a recent paper (Light-fuelled freestyle self-oscillators, https://www.nature.com/articles/s41467-019-13077-6) has nicely shown three different light induced self-oscillation modes: bending, stretching and twisting. I am not fully convinced that the difference between the current paper and what have been reported is significant enough to support the publication of the current paper in Nature.

The authors mentioned the motion of living cilia at the beginning of the paper, which is indeed a nice example. However, the authors fail to show the significance of the biomimetic motion achieved by LCE structure created in the study. The linkage between the demonstrated motion and the real applications mentioned by the authors (such as soft robotics, biomedical devices) is relatively weak, though Fig. 4b tries to relate the actuation to soft robotics applications. One minor question related to these: Figure 4 has shown more simulation results than experimental demonstrations. Why is that?

Compared to self-regulated motion of a single structure, collective motion of the systems are more interesting and much less studied in the past, according to my knowledge. However, unfortunately, the discussions of the collective motion of the self-regulated system is not thorough and not much insight has been really generated.

Referee #3 (Remarks to the Author):

This manuscript demonstrates light-responsive microposts that can be actuated to perform complex motions, triggered by UV-illumination. The microposts are made by standard micromoulding processes from existing liquid-crystal-based materials that include azobenzene as the light-switch. Key to the nature of the motion is the relative orientation of three non-colinear axes: that of the molecular alignment, that of the geometrical structure (i.e. main axis of the microposts), and that of the light direction. Varying these, induces different motions, including non-reciprocal motion. In addition, the manuscript shows that the motion can be steered by varying intensity of the illumination, micropost geometry, temperature, and irradiation intervals/duration.

The manuscript is convincing; results support the conclusions, and methods are well described. Experimental work is combined with numerical computations – the results compare well, and the numerical model has been used both to understand and to direct experiments.

The proposed approach is elegant, simple, and effective – the possibility of achieving different types of motion depending on the relative orientation of the three axes mentioned has not been shown before as far as I know, perhaps because most of the work on these and similar light-responsive materials have been done with thin film structures (for which this will be hard to realize, if not impossible) rather than the 3-D microposts presented here. This makes the approach novel. The manuscript triggers many novel ideas and may be important for future applications in soft robotics, medical applications, and energy materials, and it will be an inspiration for scientists working on light-responsive materials and structures.

My conclusion is that the manuscript can be acceptable for Nature. I do have some comments / questions to be addressed.

• Time constant in experiments: the manuscript mentions a time constant of about 9 s of the azobenzene crosslinker (see supp. Figure 4); however the timescale of the actuation might be different (likely much larger), since this depends on molecular structure (e.g. crosslink density), geometry, light intensity, etc. Indeed, a timescale of minutes is mentioned (line 173). What would be the limit here? For speeding this up, could still the same material system be used? This is important for some of the applications mentioned.

• Time constant in computations: the SI mentions a relaxation time of 120 s (line 262, SI). How was this determined? Fitting with experiments? It seems, indeed, that the time-dependent behavior is captured well by the model, from Video 6 for example where the experiment and the computation seem to move synchronously. Are we indeed looking at the same timescales for the experiment and the computation here, or has any scaling been done?

• Stiffness. The manuscript does not mention an experimental (shear) modulus (but I may have missed it) – is this known? In the computations, a shear modulus of 570kPa has been used (SI, line 242). This is relatively low for a structure that may need to do mechanical work (at least that would be needed for some of the applications mentioned). Do the authors have an idea of the work that can be performed by the actuators? What forces could they apply / resist?

• Finally, the actuators indeed can make complex motions. In all examples shown however, these are start-stop motions, that is, the motion is not perpetual unless the light source is switched on and off. Would it be conceivable to design structures with perpetual self-sustained motion (e.g.

oscillation) under the influence of continuous illumination? The manuscript starts with the example of cilia that show this type of non-reciprocal oscillatory motion.

Referee #4 (Remarks to the Author):

Novel opto-mechanical cilia actuator which can demonstrate complex motion, as a function of illumination direction and intensity. Interesting methods for fabrication of built-in anisotropy in liquid crystal material in each cilia of the array, which then demonstrates some unique behavior. These results are exciting and novel development in the field.
Data analysis and methodology are robust and complete.
Can the author answer the following questions please.
Page 3, figure 1d, what is the means of magnetic alignment of the molecules in the material ?
Page 4, lines 122, why was an angle of 45 deg selected for the alignment ?
Page 4, lines 132, is the effect on absorption a photo-bleaching effect, please clarify, this change in absorption characteristics.
Page 5, lines 168, when the UV light turns off, does the reaction continue due to diffusion of molecules which are photo-activated within the polymer ?
Page 6, line 206, with these high light intensities of 115mW/cm2 after actuation by light, is there any hysteresis present ? For example, from thermal expansion of the layers due to heat input from the light absorption ?
Page 7, lines 269, is there an optimum range of temperature for operation of the asymmetric motion of the cilia ?
Page 8, line 305, do these wave like motions have anything in common with cilia motion in clams and oysters ?

Author Rebuttals to Initial Comments:

Response to Reviewers

Reviewer comments are set on grey background, the responses to the comments are shown in black, and the newly added text in the revised manuscript and SI is set on yellow background.

Referee #1:

Reviewer comment: The authors of the article have demonstrated an interesting self-regulated system using liquid crystal elastomer microposts. The misalignment among the axial direction of the micropost, liquid crystal orientation and the light direction leads to self-regulated motion of the system. Collective motion of multiple microposts have also been investigated. The authors have also conducted numerical simulations of the dynamic behaviors of the system, and the simulation results can quantitatively capture the complex behaviors of the system. It is a very nice piece of work and the studies done by the authors are careful and systematic.

Response: We are glad the reviewer finds our self-regulatory system interesting, and we thank the reviewer for the positive comments on the quality and systematic nature of our work, as well as for highlighting the quantitative agreement between our simulations and experiments.

Reviewer comment: However, I fail to find an extremely strong point that make the presented work truly outstanding.

Response: We appreciate the opportunity to further sharpen the key features of our system and clarify the remarkable aspects of this work. Programming deformations at the microscale is fundamentally challenging, if one aims for deformations that go beyond simple contractions or bending. While 3D/4D printing, architected materials, and chemical reprogramming of materials have led to tremendous progress in the design of soft and useful macroscale actuators, their successes have really only marginally penetrated to length scales below 0.2 mm, because of difficulties in fabrication and a lack of control over deformation trajectories. So far, the intuitive response of researchers to this problem has been to create systems of more complexity: adding more stimuli, providing stimuli more locally, or adding more and different materials into multi-layer composites. The resulting microscale actuators are usually operationally cumbersome and still show a limited range of motion.

In this context, the novelty in our system is both conceptual and practical: the unique (and unprecedented so far) requirement that we introduced in our design, *i.e.* to create a compositionally uniform microstructure in which three principal axes—molecular anisotropy (***M***), geometric axis (***G***), and light direction (***L***)—are non-colinear, integrates the optical, chemical, and mechanical dynamics into a continuous series of symmetry breaking events, where the propagating order-to-disorder transition front shapes and reorients an evolving bimorph. The resulting trajectories comprise various deformational elements—right- and left-handed twisting, light-seeking or light-avoiding bending, and combinations thereof, with drastic implications for pathway control. Each pathway results from feedback among the evolving opto-chemo-mechanical behavior of the system. This iterative feedback and the resulting trajectory of motion can be controlled and shaped into a nearly indefinite diversity of actuation pathways far beyond any capabilities of current (micro)actuators. One can choose any position as the endpoint by using different light intensities, and even arbitrarily choose pairs of starting and end-positions, and cycle along non-reciprocal trajectories of different deformational elements, all displayed by the same, single-material microstructure in a size range of 10-100 μm.

The iterative, but continuous, cycles of symmetry breakings increase in complexity for systems containing multiple posts. In 2D arrays, the dynamic behavior of one pillar will affect the propagation of light in the sample and thus affect the mechanical deformation across the ensemble. These

responsive, cooperative interactions among the posts leads to dynamics, which, to the best of our knowledge, has not been reported for synthetic systems. We thank this reviewer for acknowledging below that such a collective behavior is unique and not explored so far. We have now significantly expanded upon the cooperative interactions of communicating microposts, by providing new experiments and corresponding theoretical description in the revised manuscript (see details in the answers to specific comments provided below).

Because of its minimalistic nature, our system is easily scalable into different materials systems (LCEs, hydrogels, crystals, …) and utilizing different directional stimuli. Practically, even large arrays of micropillars can be easily and rapidly fabricated by molding, while the use of a single and static light-source makes it operationally simple.

Reviewer comment: Detailed comments are given below:

Many self-oscillation modes have been demonstrated in the literature and many of the previous examples are indeed based on light responsive LCEs with the associated mechanism as opto-chemo-mechanical coupling. I understand that the specific self-oscillation modes in the paper are different from previous studies. However, the major novelty of the study is not very clear to me. In another word, what really makes the paper outstanding? The authors claim the opto-chemo-mechanical feedback is unique. But, in my opinion, the mechanism is not really too different from the self-oscillation caused by the self-shadowing effects widely explored in the literature. For example, a recent paper (Light-fuelled freestyle self-oscillators, https://www.nature.com/articles/s41467-019-13077-6) has nicely shown three different light induced self-oscillation modes: bending, stretching and twisting. I am not fully convinced that the difference between the current paper and what have been reported is significant enough to support the publication of the current paper in Nature.

Response: There are several significant differences between this study and previous work. Below, we list these differences, which highlight our new findings.

The motions of our 3D microactuators arise from the highly integrated feedback that spans across and integrates optical, chemical and mechanical energy domains: The resulting motion displays spatially and temporally more complex dynamics than self-oscillation. While self-oscillatory and self-shadowing systems do have certain elements of feedback—a delay in response after initial perturbation—and can produce interesting behavior, our work is fundamentally different from such (mostly 2D macroscopic) systems in both the dynamics that govern bimorph evolution and the diversity, complexity, and iterative tunability of a nearly unlimited set of non-reciprocal motion pathways.

(1) The novel design concept significantly expands accessible states and trajectories: Self-oscillators generally switch back and forth between specific endpoints (*i.e.*, fixed points), while this system sweeps out a continuous path of motion and shape-changes. This behavior is a direct result of the novel multi-level feedback and the symmetry breaking that was enabled by our system's design. Namely, the three principal axes, ***MGL*** are not coaligned. The resulting motion trajectories are not specific self-oscillation modes analogous to the twisting, bending, and stretching oscillations in other systems, but rather examples of how a pathway can be constructed in detail by programming how each step of bimorph evolution progresses to the next, with exquisite control over the pathway *via* small changes to any of the numerous system features. This continuous progression of states is completely unlike anything reported up to now, and enables far more diversity and complexity of pathways to be programmed for a given structure. Non-reciprocity emerges naturally from this mechanism, since pathways are determined by the series of individual steps rather than by the two endpoints. *We also note that self-shadowing is neither necessary nor sufficient for this mechanism.* In fact, our structures do not bend to block light (shown as an operating principle for self-shadowed, self-oscillating systems), and we would argue that they rather undergo 'self-exposing' during the unique twisting motions.

(2) **Self-regulation provides spatial control:** Our ability to orient the nematic director along any direction, along with the controllable order-to-disorder propagation in posts with non-aligned ***MGL*** axes provides a modular system in which specific interventions (light-intensity and direction, operating temperature, …) allow one to precisely sample various positions along a controlled trajectory. For self-oscillators, in contrast, the 'freestyle' in the title of the cited paper (Light-fuelled freestyle self-oscillators. *Nat. Comm.*, **2019**, *10* (1), 1-9.) indicates, and the main text confirms, that the level of control over deformation trajectories is limited. Self-oscillators are typically restricted to a single type of deformation, and it is very important to note that the *three different deformation modes* described in this elegant work by Priimagi and Zeng—bending, contraction, and twisting—are achieved *for three different self-oscillators* with distinct orientation of molecular anisotropy. The more sophisticated freestyle-type oscillations described in the manuscript require an increase in degrees of freedom, which is achieved by hanging the thin films on a string: deformation of the film by local irradiation, causes the center of mass to shift, the film to move out of the beam path, allowing for relaxation of deformation, shifting of the center of mass back to its original position and renewed exposure to irradiation. In contrast, in our design, it is *the same uniform microstructure that can display any of right- or left-handed twisting, light-seeking or light-avoiding bending and move along multiple, well-controlled non-reciprocal trajectories*.

(3) **Global directional stimuli make the system operationally simple:** Most light-based self-oscillators are macroscale thin-film systems, where oscillations are restricted to defined regions of the parameter space. Film orientation and exact position of the light source require careful optimization to observe sustained self-oscillations. Usually, the spot size of irradiation is (much) smaller than the macroscale 2D film size (for the cited paper this is: film size = 3.5 × 3.5 × 0.05 mm, laser = 180 mW, spot size 1 = 20 µm, spot size 2 = 2.2 mm). In contrast, our actuators operate under global directional illumination.

(4) **The reported array dynamics is fundamentally different from coupled oscillators:** Cilial carpets are often modelled as ensembles of coupled self-oscillators. The fundamentally different actuation and self-regulation mechanism for our 3D microactuators, however, also changes how our pillars coordinate and move in ensembles—the complexity of motion both for each single pillar and coordinated as an ensemble goes far beyond collective patterns in cilial carpets that arise from locally varying phases and frequencies of otherwise similar oscillations. Moreover, the self-organization seen in strings of pillars shown in our paper, where stable bimorphs form (and thus no repeated actuation is observed) is a further example of how the concept of programmed local symmetry breaking provides access to fundamentally new behaviors that have not been reported before. In contrast to cilia and the described 3D microactuators, traditional 2D thin-film light-based self-oscillators are fundamentally unsuited for operation in large 2D arrays. Mechanical coupling between a pair of parallel self-oscillators (*Nature Materials*, **2021**, *20*, 1702–1706) is possible, but because each oscillator operates on self-shadowing of a light beam—shadowing others in the process—no stable irradiation field, which is necessary for sustained self-oscillation, is possible for subjacent rows of actuators.

We now highlight all these points more explicitly in the conclusion of the revised manuscript page 11, lines 402-413:

> *"To conclude, we present a strategy for programming various self-regulated, stroke-like dancing trajectories in a single, compositionally uniform microstructure fabricated by a simple molding procedure. The self-regulatory behavior is fundamentally different from existing feedback systems: thanks to the 3D non-coaligned **MLG** axes, light propagating through the material generates a transient, dynamically evolving bimorph with increasingly complex symmetry-breaking along the front, determined by iterative cycles of opto-chemo-mechanical feedback and specifying a motion pathway composed of many different deformation types—composites of twisting, bending, light-seeking, and light-avoiding—with diversity, complexity,*

and fine tunability. The resulting range of motion and pathway control cannot be achieved with existing approaches that involve complicated multi-material architectures, 3D printing, or direct manipulation, especially for 3D structures in the 10-100 µm size range. Our simulations quantitatively capture these multilevel feedback dynamics, allowing us to theoretically predict and experimentally program the spatiotemporal behavior of nearly infinite different actuation pathways."

Reviewer comment: The authors mentioned the motion of living cilia at the beginning of the paper, which is indeed a nice example. However, the authors fail to show the significance of the biomimetic motion achieved by LCE structure created in the study. The linkage between the demonstrated motion and the real applications mentioned by the authors (such as soft robotics, biomedical devices) is relatively weak, though Fig. 4b tries to relate the actuation to soft robotics applications.

Response: We appreciate the opportunity to further sharpen our argument on why the comparison with the deformation behavior of natural cilia and flagella is useful. Such 'living' actuators have inspired researchers for a long time, posing a challenge for synthetic systems with regard to mobility at the microscopic level, the non-reciprocality of the motion, the speed of 'beating' (often in tens of Hz to kHz), and the utility for mass and fluid transport. As we detail in the introduction, many systems have been reported to date; some excel in certain features, where others have impediments. However, for us the multi-scale self-regulation in cilia motion that governs and spans the molecular to cilial to ensemble scale (see *e.g. Nat. Rev. Phys.* **2020**, *2*, 74 and *Science*, **2018**, *360* (6387), eaar1968) is a feature that deserves more attention and that goes beyond simple biomimetics focused on performance benchmarks. Across materials sciences, researchers acknowledge that self-regulation and communication between ensembles of materials are essential to take the next step towards life-like or intelligent matter (see *e.g.* ´The rise of intelligent matter´. *Nature*, **2021**, *594* (7863), 345-355). Programming self-regulated motion at the microscale is fundamentally challenging and we believe that cilia present an inspiring example of how self-regulation across scales translates into motion, *in particular non-reciprocity of motion*. It was not our purpose to create microactuators, whose beating frequency, efficiency for fluid transport, or even the exact shape of the power and recovery stroke match those of natural cilia. We use these biological systems as an inspiration, to borrow from them the fundamental design principles that can guide us in the creation of materials and devices with properties that often surpass the natural systems. In fact, the presented actuators show hallmarks of some complex systems found in biology, including interactions and communication within ensembles, complex functions such as non-reciprocal motions, the ability to switch between multiple states and the sensitivity to perturbations that can cause critical transitions. In our case, the complexity and programmability of diverse, non-linear motion trajectories, which are achievable by the same, simple, compositionally uniform structure, is, to our knowledge, unparalleled in the movement of cilia or any synthetic microactuators.

Regarding the question of real-world applicability: the high level of control, ease of fabrication by molding into any desired shape as well as simplicity of operation with a static light source, and theoretical predictability make the presented design approach ideal for soft robotic applications, particularly at the microscopic (~10-100 µm) level, unachievable using most of the existing fabrication strategies. We demonstrate the applicability of our approach in achieving motion complexity in a single micropost, micro-arrays, as well as free-standing jointed soft actuators, which we believe show great promise in realizing useful and complicated motions displayed by the same structure.

We have updated the conclusion to include a comparison with natural cilia and potential applications of our system, page 12, lines 417-433

*"Furthermore, this self-regulated bimorph dynamics has dramatic implications for eliciting complex collective behaviors in microstructure arrays, where **MLG** reorientations involving*

additional geometrical axes (G_{array}) lead to distinct position-dependent symmetry-breaking and unique motion pathways for each micropost, The interpillar communication and multilevel propagation dynamics we demonstrate reveal the fundamental scalability and predictability of the designed feedback mechanism beyond a single microstructure, and provide means to control the collective behavior in microstructure ensembles. The observed emergent behaviors, such as bistability, stable wave-like patterns, and sensitivity to small perturbations, are typically hallmarks of complexity[47] in multi-component systems that rely on molecular-scale, diffusion, or flow-limited processes such as chemical reaction networks[48-50] or even chemo-mechanical actuators[27,28], but here complexity emerges from the simplicity of the single-material photo-responsive system. The design concepts introduced herein also lead to bird-like and other complex programmed motions in freestanding jointed single-material microstructures with multiple non-aligned $G_{segment}$ axes. This vast design space for individual and collective motions is potentially transformative for fields ranging from soft robotics, micro-walkers, sensors, and cell culture scaffolds to robust information encryption systems where information encoded in an array can be read out by an infinite number of different dynamic patterns evoked by different illumination directions, intensities, durations, intervals, as well as wavelengths and polarizations."

Reviewer comment: One minor question related to these: Figure 4 has shown more simulation results than experimental demonstrations. Why is that?

Response: As the calculations demonstrate nicely the potential and usefulness of the reported approach, we had put the emphasis on simulation results in the **old Fig. 4**. However, in the revised manuscript, we now significantly expand on the experimental results and divided **old Fig. 4** into two separate figures: the **new Fig. 4** (reproduced below in its entirety) is now focused on micropost arrays and their collective behavior, and the **new Fig. 5** (reproduced below in its entirety) focuses on free-standing and attached jointed microstructures and provides additional experimental results in **Fig. 5.a-ii** that match well with the predicted behavior. Moreover, we now include an additional simplified discrete model for pillar arrays (SI Model **3**, SI section 2.3, page 11-12), complementary to our **Model 1** (SI section 2.1, page 8-9) using finite element approaches, to capture the emergent deformation behavior in larger scale micro-arrays. Though these two models are constructed under different assumptions, both produce consistent results in smaller systems, indicating the robustness of our mechanism and its applicability for a broad range of structure geometries and arrangements.

The combination of experiment and theory provides a powerful means to advance materials sciences, yet this interdisciplinary work is often challenging and is not pursued often enough. We strongly believe that it is important to show simulation results, especially because experiment and model agree quantitatively, and that in our case the theory is crucial to both understand the mechanisms governing the experiments and explore a large design space to guide future designs for specifically targeted performance and functions.

Reproduction of **Manuscript Fig. 4**, page 9-10, lines 330-346:

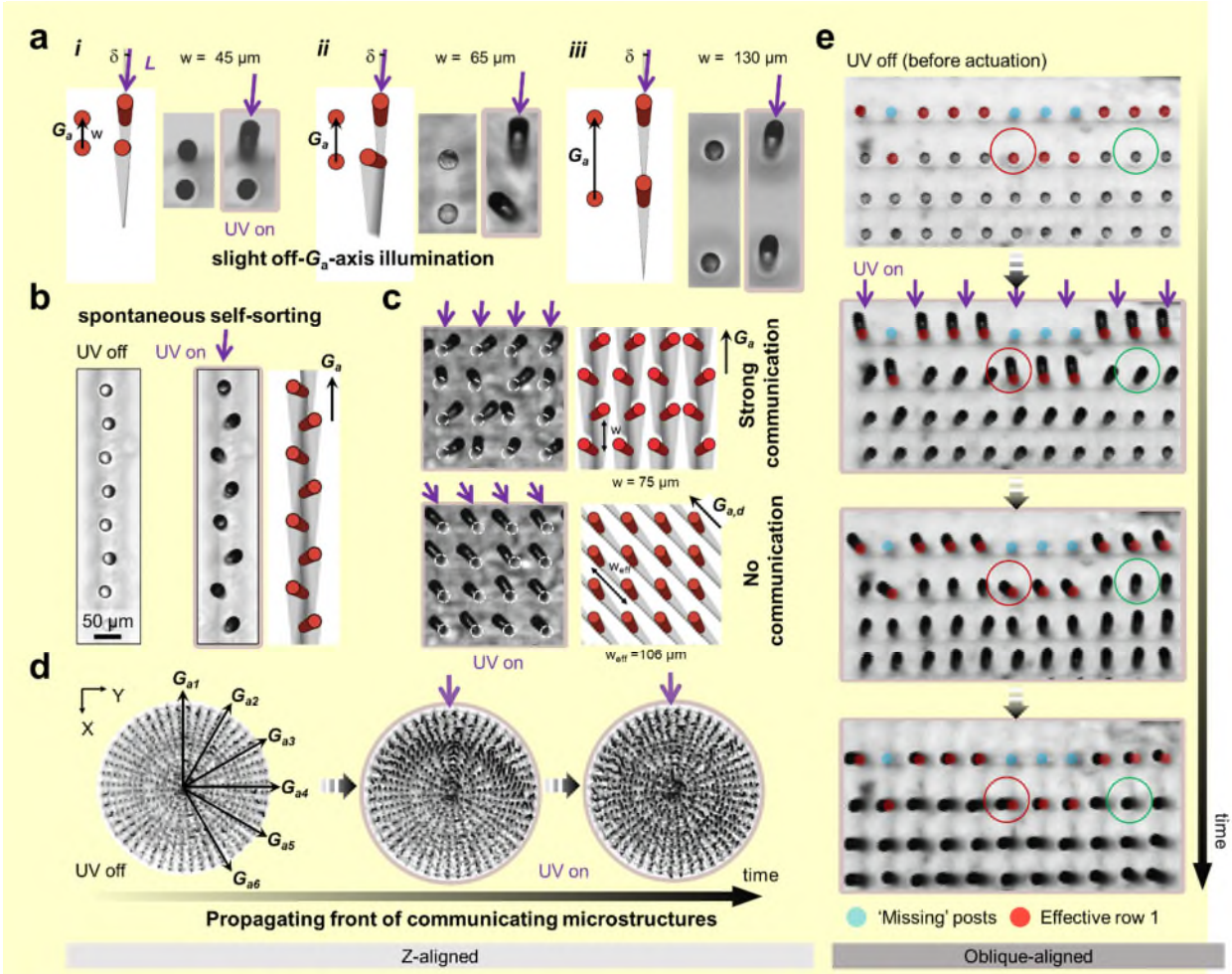

Figure 4 | Collective self-regulated deformation dynamics in arrays of microposts. a. Simulation (left) and experimental (right) results of the light response of pairs of microposts, when the illumination direction, ***L***, forms a small angle, d, with the pair axis, G_a, illustrating how different interpost spacings, *w*, influence the deformation trajectory of subsequent posts: *i* – small interpost spacing *w*=45 µm; *ii* – at defined, intermediate interpost spacings (*w*=65 µm in the presented case), the most pronounced communication and collective behavior is observed; *iii* – at large spacings (*w*=130 µm in the presented case), uncorrelated, identical light-induced bending of both microposts occurs. **b.** In appropriately spaced strings of microposts, distance- and location-dependent symmetry-breaking results in spontaneous self-organization into stable patterns in the form of an undulating line upon irradiation. Such pattern formation is well captured by our models (shown on the right). **c.** As the angle of irradiation changes within a 2D-microarray, effective interpillar distances vary, which changes the resulting deformation and self-organization behavior, corresponding to coupled and decoupled uniform light-seeking motions when light comes along the nearest neighbor (G_a, *w*= 75µm), or diagonal ($G_{a,d}$, *w*=106 µm) directions, respectively. **d.** Formation of a complex travelling wave of locally interacting posts in a radially arranged micro-array, demonstrating a rich ensemble dynamics. **e.** Amplification of engineered 'defects' in arrays of oblique-aligned microposts: missing microstructures alter the local illumination conditions and inter-pillar spacing and dramatically change the deformation trajectories of the posts around them and thus the overall ensemble dynamics.

Reproduction of **Manuscript Fig. 5**, page 11, lines 384-400:

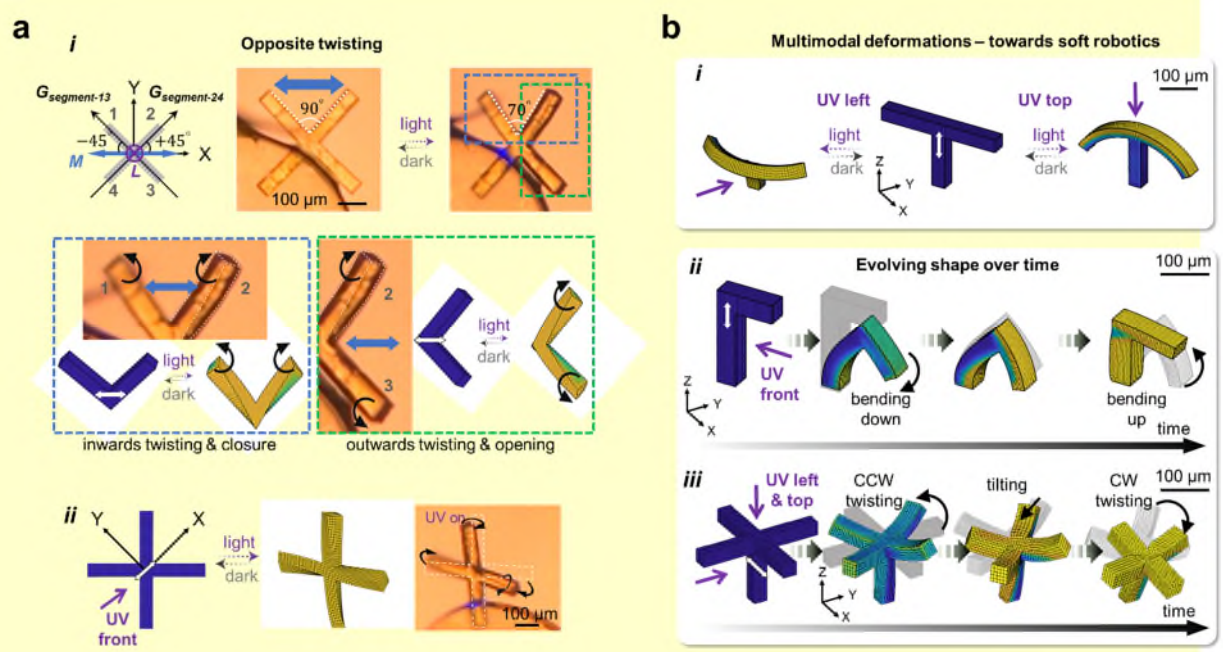

Figure 5 | **Higher-order self-regulated dynamics in jointed soft microactuators.** Single-material soft robotic elements of X-, T-, L-, or palm tree-shapes show cooperative deformation behaviors in which the deformation modes of each stem/arm work in concert to produce highly non-linear, yet easily programmable bird-like flapping, 'stirring', grabbing, or bending motions. **a**. *i*) In a free-standing X-shaped actuator containing two perpendicular structural axes $\boldsymbol{G}^{13}_{segment}$ and $\boldsymbol{G}^{24}_{segment}$, which form +45° and –45° with the uniform director orientation, ***M*** (shown as a blue double-arrow), bending and twisting motions of opposite direction can be invoked for different arms within the same single-material, compositionally uniform microstructure. Magnified photographs and corresponding theoretical simulations depicting the motion of the top two and the right two segments of the structure are shown below in a blue and green insets, respectively. *ii*) with one arm being the anchoring spot, the twisting of $\boldsymbol{G}^{24}_{segment}$ couples to the twisting/rotation of the $\boldsymbol{G}^{13}_{segment}$-axis, demonstrating amplification of the sway motion through the arms in both simulations and experiments. **b.** Our theoretical simulations underscore these principles: *i*) T-shape with global vertical molecular alignment that undergoes distinct deformations for different light directions. *ii*) L-shape actuator with global vertical molecular alignment, illustrating a programmable movement sequence of bending down and upwards in a single UV-actuation period as a travelling light front propagates through the structure. *iii*) Palm tree-shape actuator with oblique alignment, illustrating a progressive counterclockwise and clockwise twisting accompanied by the closure and opening of the arms.

Based on the insights on collective behavior (see below) and the additional experimental data, we have adapted the main text of the manuscript, page 10-11, lines 348-400:

> *"In free-standing jointed compositionally uniform microstructures, the presence of multiple geometrical axes (in this case* $\boldsymbol{G}_{segment}$*, the principal symmetry axis of each constitutive part) provides additional opportunities for cooperative symmetry-breaking and bimorph evolution, which can give rise to complex deformation patterns such as stirring, bowing, or bird-like motions. These constituent segments along different directions will each have a distinct relative* $\boldsymbol{G}_{segment}\boldsymbol{ML}$ *orientation and thus exhibit distinct local symmetry breakings and corresponding motions (Supplementary Figs.* ***31-33****, Video* ***20****), even with, in the simplest case, a globally uniform molecular alignment (****M****) and a single static light source (****L****). As demonstrated in a compositionally uniform X-shaped actuator consisting of four arms with an oblique mesogen alignment, in which the global molecular alignment* ***M*** *is uniformly oriented*

within the entire structure, but forms +45° and –45° respectively with the arms' structural axes $\boldsymbol{G}^{13}_{segment}$ *and* $\boldsymbol{G}^{24}_{segment}$*, when illuminated perpendicular to the microstructure plane (Supplementary Video* ***21****), the resulting programmable deformations include mutually opposite right- and left-handed twisting and bending of the arms reminiscent of crawlers or the wing-warping/twisting necessary for bird flight. The helicity and extent of twisting and closure/opening or out-of-plane movements of the arms can be judiciously chosen through variations of relative orientations of* ***L****,* ***M****, and geometric axes of each segment* $\boldsymbol{G}_{segment}$*. Furthermore, if one end of the arm (*$\boldsymbol{G}^{13}_{segment}$*) now serves as an anchoring point, a twist of* $\boldsymbol{G}^{24}_{segment}$ *fully coupled to the motion of* $\boldsymbol{G}^{13}_{segment}$ *is observed, and as a result such twisting is greatly amplified by the extended arm having accompanied rotation of a much greater displacement (Supplementary Video* ***22****). This implies that such actuators can serve as micro-joints/hinges with the ability to control a variety of motion trajectories of macroscale pieces. In contrast, thermal heating of the X-shaped actuator shows only one deformation—a direct shrinkage along the molecular alignment to a 'slender'-X without undergoing any twisting (Supplementary Fig.* ***34****). Our computational method allows us to further explore a library of combinations of* $\boldsymbol{G}_{segment}$***ML*** *and show deformations including 'stirring', catching, or releasing cargo (Supplementary Video* ***23****). As an illustration, a compositionally uniform T-shaped actuator with global vertical director alignment (Fig.* ***5b****) will undergo multiple deformations depending on the light direction, due to formation of different transient 3D bimorphs with the 'activated' (yellow-to-green) region exerting tensile/compressive forces on the 'non-activated' (blue) region. Moving onto the dynamic bimorph regime, through the traveling order-to-disorder transition, such behaviors are also programmed in time: i) In a vertically-aligned L-shaped actuator (****Fig. 5c-i****), upon irradiation from the front, the lever first bends down towards the light, then rises again, all in a single UV-actuation period; ii) in a more complex palm tree geometry with oblique alignment (****Fig. 5c-ii****), the levers first bend up accompanied by a counterclockwise rotation due to the coupling to the twisting stem, and then open up with a clockwise rotation. Non-symmetrical movements of different arms can be readily achieved by shifting the illumination direction away from the structure symmetric axes or having off-axis director orientation (Supplementary Fig.* ***35****). The ramifications for microscopic soft robots capable of a tremendous set of motions are immediate and numerous."*

And is also reflected in the updated caption of Supplementary Figure 35, page 37:

"Supplementary Figure 35 | *The motion of the two respective arms of a jointed microstructure of V-shape, in which the molecular alignment is offset with regard to the X-axis, creating two segments, in which* ***M*** *is oblique with respect to* $\boldsymbol{G}_{segment}$*, but different. As a result these two segments (arms) exhibit stroke-like deformations either toward (*$\vartheta \leq 45°$*) or away from the light (*$\vartheta \geq 60°$*) for out-of-plane irradiation (UV 1 and UV 2). Similarly, the arms will behave differently for in-plane irradiation (UV 3 & UV 4). Please also refer to Manuscript Figure* ***3e*** *for a detailed discussion on the influence of director tilt and different illumination directions in a square micropost on the post´s deformation behavior."*

The additional experimental data of **Fig. 5.a-ii** on free-standing jointed actuators can be found in the Supporting Information, page 39, Supplementary Video 22 :

*"****Supplementary Video 22 |*** *If an X-shaped actuator is anchored at the end of one segment, its twisting motion amplifies through the horizontal branching arm. At the same time, twisting of each segment is observed (Manuscript Figure* ***5a,ii)****."*

Reviewer comment: Compared to self-regulated motion of a single structure, collective motion of the systems are more interesting and much less studied in the past, according to my knowledge. However, unfortunately, the discussions of the collective motion of the self-regulated system is not thorough and not much insight has been really generated.

Response: We appreciate that the Reviewer finds the collective motion interesting. And indeed, we do see a lot of wealth in the micro-array systems when higher-order dynamics emerge from the communication from multiple geometrical axes and the local dynamic symmetry breakings. We have expanded significantly on the collective motion in the manuscript in both simulation and experiments and added a **new Fig. 4** (reproduced above), an additional simplified **Model 3** (SI Section 2.3, page 11-12), and Figs. S25-29, reproduced below, to thoroughly investigate the fundamental two-post interactions and showcase the complexity we can easily reach in strings of microstructures and 2D arrays with our strategy.

We have added the following text to the manuscript page 8-9, line 285-326:

"As one expands the system from a single micropost to strings of microstructures or 2D arrays (produced by a simple molding procedure), additional symmetry axes (degrees of freedom) are added to the system, which in the simplest case of a 1D array can be captured by the array axis $\boldsymbol{G_a}$ *defined in terms of a string direction and interpillar distances, w. We explored the potential for dynamic pattern evolution and emergent communication between the microstructures in such a system using a string of circular microposts with z-aligned mesogens (**G** and **M** colinear within each pillar, Fig. **4a**) under experimental conditions that favor stable bimorphs (as in Fig. **2**; Supplementary Fig. **8**). If* $\boldsymbol{G_a}$ *and **L** are perfectly aligned, one would expect only bending towards the light (along the string axis) with rapidly decreasing amplitude. However, we hypothesized (as schematically presented in Supplementary Fig. **25**) that with even a small misalignment between* $\boldsymbol{G_a}$ *and **L** (shown as angle d), the first pillar would bend slightly out of line, leading to asymmetric exposure of the next pillar and creating a bimorph that bends out of the string axis in an opposite direction, with bending amplitude and symmetry breaking amplified along the string in a distance- and location-dependent manner. To capture such a unique collective response in pillar arrays, we developed a simplified discrete model that considers how interpillar communication changes what parts of neighboring microstructures get illuminated and when upon directional light exposure (Supplementary Model **3**, Supplementary Fig. **26**). Our simulations, confirmed by the follow-up experiments, show that in pairs of z-aligned microposts of different interpost spacing w (w=45, 65, or 130 µm), for a small angle, d, between* $\boldsymbol{G_a}$ *and **L**, symmetry breaking arises at w=65 µm, while at short distances no actuation of the second post occurs and at long distances 'decoupled', identical deformation of the posts is observed (Fig. **4a**). In longer strings, such distance-dependent symmetry breaking leads to a stable and repeatedly reproducible wave-like pattern (Fig. **4b**, Supplementary Video **13**), a behavior accurately captured by both our finite element simulations (Supplementary Fig. **27**, Video **14**) and a simplified mathematical model (as shown in Fig. **4b**, right). The spontaneous asymmetry amplification endows the system with a high sensitivity to any* $\boldsymbol{G_aLM}$ *noncolinearity and access to drastically different self-sorted patterns (Supplementary Figs. **28&29**, Video **15-16**). The degree of interpillar coupling and thus self-organization depends strongly on the magnitude of misalignment, d, between* $\boldsymbol{G_a}$ *and **L**, most effectively demonstrated in a 2D square array of microposts containing* $\boldsymbol{G_a}$ *(axis along the nearest neighbor) and* $\boldsymbol{G_{a,d}}$ *(direction along the diagonal) axes. As the array is illuminated along the* $\boldsymbol{G_a}$ *or* $\boldsymbol{G_{a,d}}$ *direction, the effective interpost spacing changes, thus enhancing or suppressing the interpost communication (Fig. **4c**, Supplementary Video **17**).*

*We further note that under conditions that allow for dynamic bimorph propagation locally within each single pillar (as described in **Fig. 3**), a unique, global deformation front is expected to travel concurrently at the ensemble level (with a different propagation velocity) dependent on the effective pillar density along the light path. Indeed, we showcase in a radially arranged micro-array with z-aligned mesogens (**Fig. 4d**) that when the array is illuminated from one side, these interacting propagation fronts lead to a complex evolution of the traveling wave of the communicating posts at the ensemble level. In this radial arrangement, the multiple **G_a** axes have different relative orientations to **L**, resulting in various local hierarchical spacings along the light path and causing the complexity of the collective traveling front (Supplementary Video **18**). Moreover, if **G** and **M** are non-colinear within each micropost, one would expect that in a 2D array, the previously described 'dancing' motions of each post would adapt to and self-organize with the motion of their neighbors, with each post undergoing a unique position-dependent trajectory (Supplementary Fig. **30**). Together with programmed defects (e.g., missing pillars), one can therefore construct micropost ensembles with highly controlled, emergent time- and location-dependent deformation trajectories (Fig. **4e**). For example, two microposts (circled red and green) from the same row in the array exhibit completely different deformation trajectories yet start and end at similar states (Fig. **4e**, Supplementary Video **19**)."*

We have extended our in-house developed finite element simulations for multipost arrays, see SI section 2.1, page 9.

*"The above methodology can then be extended to arrays of posts, with equation S4 used to trace light rays through one structure and into another disconnected structure and determine what parts of the surface of each post will be obscured by neighboring posts. Such simulations predict interactions within arrays of posts similar to what was observed experimentally (Supplementary Figure **27**, Video **14**). We find that for a row of posts, we can approximate the effect of a finite-size light source in experiment with two ideal light sources (assumed to be propagating from infinity along all vectors parallel to $\hat{\boldsymbol{v}}_{\boldsymbol{l}}$) separated at an angle of ±1° from the post-to-post separation axis. The first post on the path of the incident light bends towards the light as it would in isolation. However, the second post is subject only to glancing incidence on its sides—it is unstable in the sense that a slight deflection out of the plane defined by the vertical axes of the posts and the line connecting the post bases will lead to more isomerization on that face. This will induce more contraction and further deflection out of the plane. The direction of this out-of-plane deflection of the second post will cause selective irradiation of the next (third) post from any glancing incidence but not the other. This causes the third post in the sequence to deflect out of plane in the opposite direction. This out-of-plane deflection will in turn change irradiation of the subsequent post, and the effect will propagate along the line of posts."*

Our new Model 3 can be found in SI section 2.3, page 11-12.

"Model 3: Simplified Discrete Model for Micropost Arrays

*To capture the collective response of a micropost array to irradiation, we establish a simple discrete model. We consider an array of cylindrical posts with diameter a that are exposed to UV light forming an angle β with Y-axis. Because the size of the UV light is comparable to its distance from the micropost array, we assume that the shadow formed by a cylindrical post has a long triangular shape and is characterized by its length L_{shadow} (Supplementary Figure **26a**). Note that L_{shadow} depends on many factors, for instance, the distance, size and*

collimation of the UV light, therefore in our model we treat L_{shadow} as a fitting parameter to part of the experimental measurements.

*When the array of microposts is exposed to UV light, every microstructure generates a triangular shadow whose direction is determined by light angle β. For each post, we can loop over all other posts to figure out which part of the microstructure is being shadowed by others. For the parts that are not being shadowed, the UV light penetrates l_B into the post and activates certain areas of the post (Supplementary Figure **26b**). Note that since the microposts considered in our study have a thin skin layer that does not respond to UV light, in our model the outer ring with thickness δ_{non} is also not activated. To model the equivalent bending force generated by the illuminated areas S_{light}, we introduce a local coordinate x' and y' that is aligned with the light direction. The equivalent force on the post is therefore calculated as*

$$F_{light}^{x'} = \int_{S_{light}} P_{light}\, x'\, dS_{light} \qquad (S14)$$

$$F_{light}^{y'} = \int_{S_{light}} P_{light}\, y'\, dS_{light} \qquad (S15)$$

where P_{light} is another fitting parameter characterizing how strong the posts respond to the UV light. For the sake of simplicity, we use the vector $\vec{F}_{light}$ to denote this force.

*Furthermore, since the microposts are 3D objects, their shadows are also in 3D. To address this point, we discretize the post as a stack of N disks (Supplementary Figure **26c**). We simply assume that upon activation the post deforms linearly as a tilted straight line. Then the light induced force is calculated depending on the positions of posts at each layer i, as $\vec{F}_{light}^{i}$. Compared to the disks on the top, disks near the bottom have a larger effect on the positions of the post tip. Therefore, the total equivalent force is defined as $\vec{F}_{light}^{total} = \frac{1}{N}\sum_{i=1}^{N} \frac{N-i-1}{N} \vec{F}_{light}^{i}$. Finally, we use two linear springs k_x and k_y to model the elastic resistance of the posts during bending (Supplementary Figure **26d**). The balance between light induced force and the linear springs yields the final positions of the post tips,*

$$k_x u = \vec{F}_{light,x}^{total} \text{ and } k_y v = \vec{F}_{light,y}^{total} \qquad (S16)$$

where u and v are the x and y-displacements of the post tip. Equation S16 is solved numerically for different post distributions and light directions using the Runge-Kutta method with MATLAB."

In addition, new Supplementary Figs. **25-29** are reproduced below.

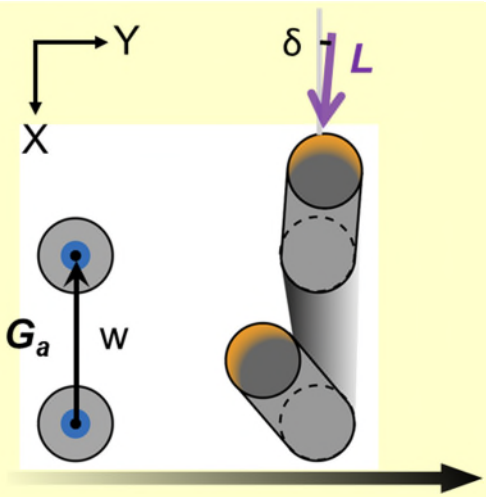

*"**Supplementary Figure 25 |** Schematic illustration of the origin of pattern formation in arrays of Z-aligned microposts (Manuscript Figure **4a**): Under experimental conditions that favor stable bimorphs, even a small misalignment between $\boldsymbol{G}_{array}$ and **L** causes symmetry breaking that can lead to starkly different deformations of posts along the array. As the first post bends towards the light along **L** with a small angle δ to the array axis $\boldsymbol{G}_{array}$, the subsequent post gets exposed to light only partially, promoting its out-of-plane bending, which gets amplified, the more the post deforms. The resulting location-dependent symmetry-breaking and deformation creates stable, self-organized patterns along the post array. Note that the velocity of propagation of the order-to-disorder front within each pillar can be different from the velocity of deformation along the string"*

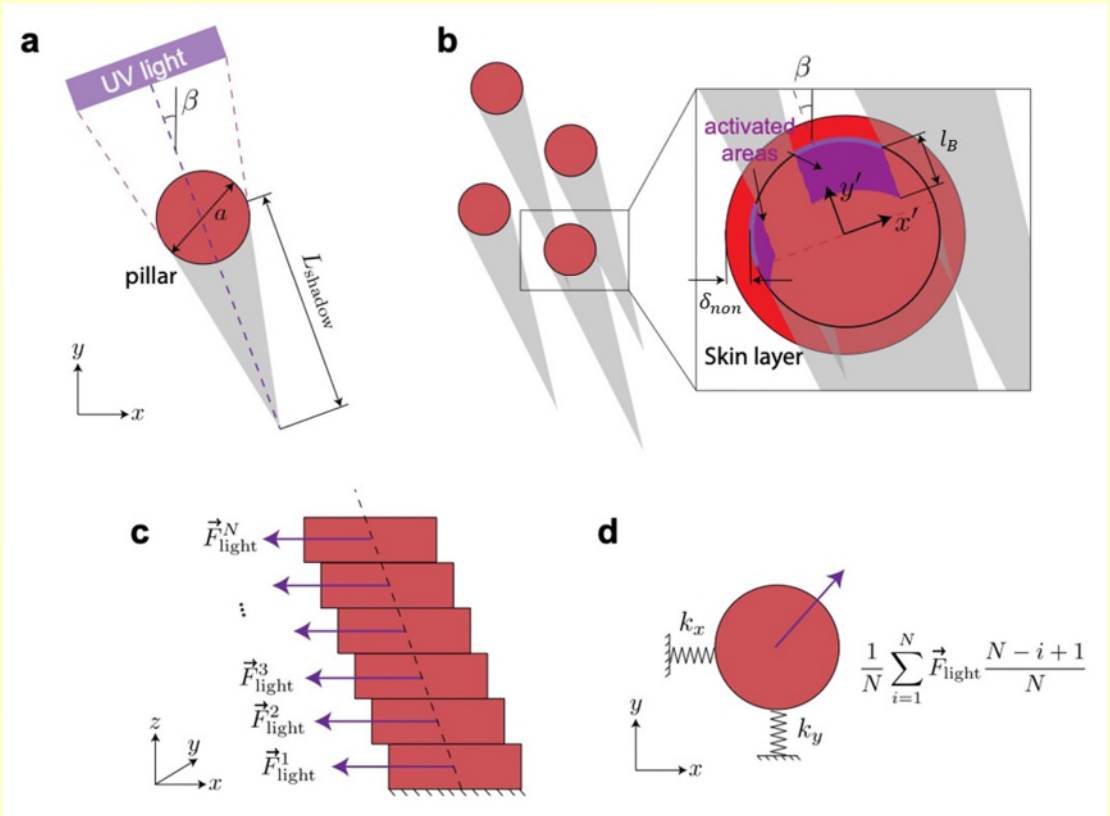

*"**Supplementary Figure 26 |** Discrete model to capture the collective deformation response of micropost arrays under UV light from different angles. **a.** The cylindrical post shades a*

triangular shadow against the UV light. ***b.*** *For each post, the shadow from other posts blocks UV light. As a result, only part of the post is activated, considering penetration depth* l_B *and a ring of non-excitable material given by* δ_{non}. ***c.*** *We discretize the post as a stack of disks and each layer exerts an equivalent light-induced activation force.* ***d.*** *The total force is balanced by two linear springs to yield the final top displacements of the posts. For more details, please refer to SI Model* ***3****, section 2.3."*

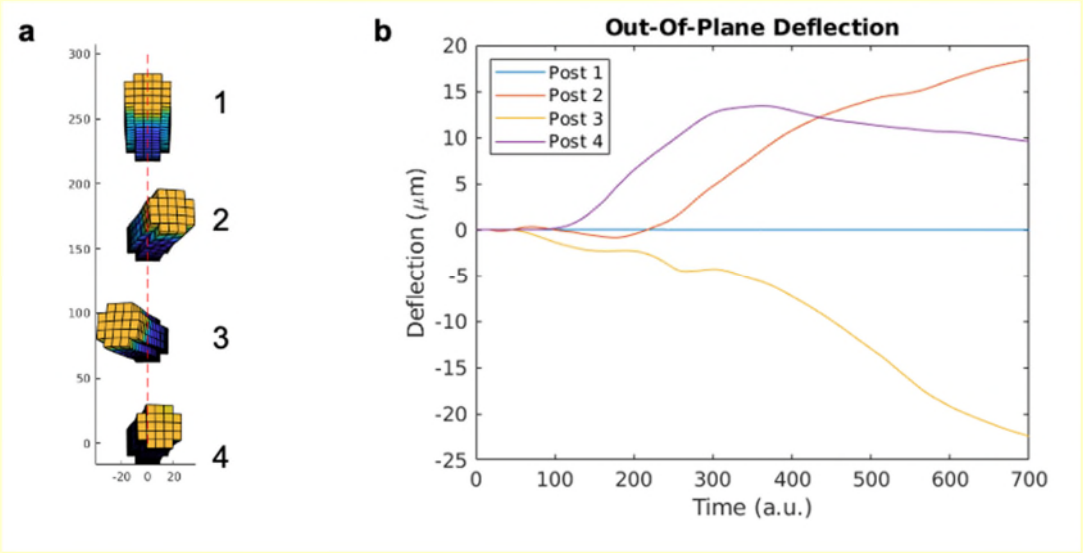

*"**Supplementary Figure 27 |** Simulated deformation of circular microposts within an array (Supplementary Video **14**). Posts are subject to irradiation from two light sources offset by ±1° offset to the array axis. Post dimensions correspond to a height of 150 μm and diameter of 30 μm, with a center-to-center separation of 78 μm along the array.* ***a.*** *The nematic director is oriented along the vertical (Z-)axis of the posts, resulting in phototropic bending. Light vectors are propagated through the finite elements as described in Model* ***1****.* ***b.*** *Out-of-plane (out-of-string) deformation through time for the four posts."*

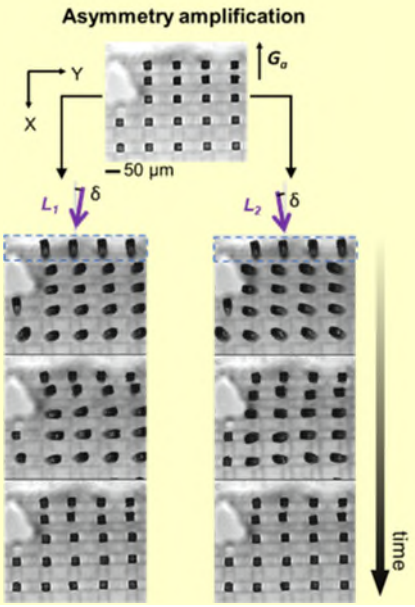

*"**Supplementary Figure 28 |** A clear asymmetry amplification effect is observed in an array of square microposts with mesogenic alignment along the Z-direction: for the same array, when light is along the X-axis with just a small negative/positive angle δ with regard to the X-axis (corresponding to **G_{ax}**), amplification of the asymmetry is observed as the amplitude of out-of-plane deformation increases along the array. As δ is very small, no noticeable difference in deformation is observed for first row of posts (marked with a blue dashed box). However, subjacent rows of posts are exposed to light asymmetrically because of inter-post communication, amplifying the deformation out of plane. Temperature 60 °C. See also Supplementary Video **15**."*

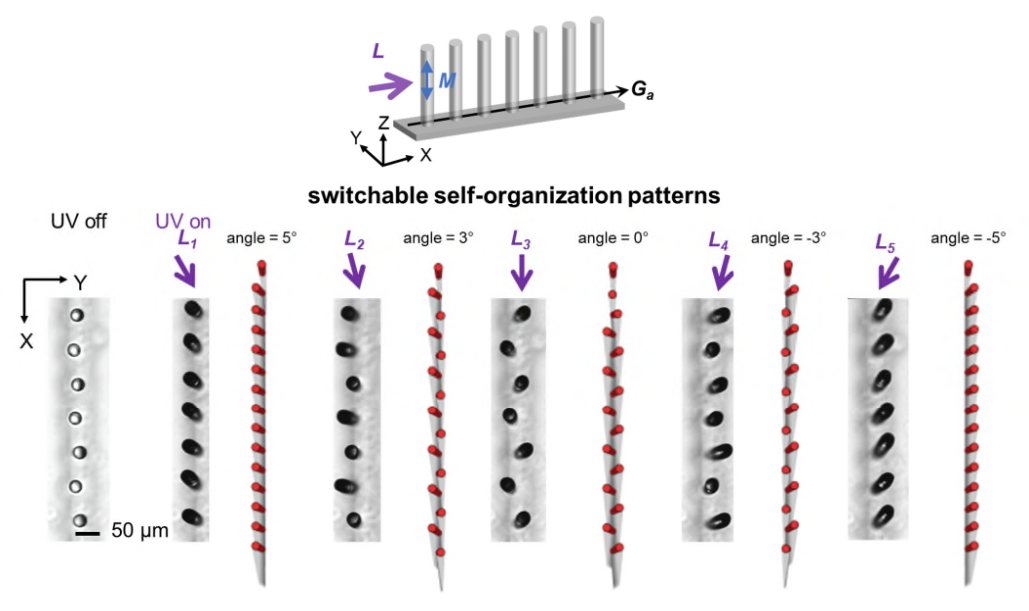

*"**Supplementary Figure 29 |** Variation of the angle of irradiation **L** with respect to **G_{array}**, creates different self-organized patterns of deformations under experimental conditions that favor stable bimorphs. While **L_1** and **L_5** show near-uniform out-of-plane bending (compare to the amplification observed in Supplementary Figure **28**), undulating wave-patterns of different accentuation are formed for angles associated with **L_2**, **L_3** (see also Supplementary Video **13**), and **L_4**. The angles of purple arrows are exaggerated for illustration purposes. See also Supplementary Video **16**."*

We now also include updated captions for Supplementary Video 13, and add new Supplementary Videos **14-18**, SI page 39:

*"**Supplementary Video 13 |** Spacing-dependent interpost-communication in arrays of Z-aligned microposts: Arrays of vertically aligned closely-packed microposts spontaneously self-organize into stable patterns in the form of an undulating line upon irradiation under conditions that favor formation of a stable bimorph with each post. Formation of such wave-like patterns is highly reproducible. Micropost diameter 25 µm; interpost spacing 65 µm along. Note that **G_{array}** and **L** are slightly misaligned (by a small angle δ, Supplementary Figure **25**, Manuscript Figure **4a** & **b**)."*

*"**Supplementary Video 14 |** Simulation results of the photoresponsive behavior of a vertically-aligned square post array (30 x 150 µm and 78 µm interpost spacing) upon illumination along the string. Posts are subject to irradiation from two light sources offset by ±1° offset to the array axis (Supplementary Figure **27**)."*

*"**Supplementary Video 15 |** In an array of square microposts, this initial asymmetry can be amplified along the array (Supplementary Figure **28**)."*

*"**Supplementary Video 16 |** Different self-organized patterns may be attained by slightly changing δ. Note that indicated angles of illumination are exaggerated for illustration purposes (Supplementary Figure **29**)."*

*"**Supplementary Video 17 |** In square 2D arrays, changes of the illumination direction from the nearest neighbor to the diagonal, changes the effective interpost distance in the array, which influences the presence or absence of inter-post communication and collective behavior (Manuscript Figure **4c**)."*

*"**Supplementary Video 18 |** Under experimental conditions that favor isomerization front propagation within each post, irradiation of a circular array of microposts creates collective deformation dynamics, in which a global deformation front travels concurrently (with a different propagation velocity) across the array shaped by the locally changing interpost spacing and different $\boldsymbol{G_a}$-axes (Manuscript Figure **4d**)."*

***Supplementary Video 19 |** Amplification of 'defects' in arrays of oblique-aligned microposts: missing posts alter the interpost spacing and dramatically change the deformation trajectories of neighboring posts and thus the overall collective deformation dynamics (Manuscript Figure **4e**). Note the similar behavior of the 'effective first row' (denoted by red circles).*

Referee #3:

Reviewer comment: This manuscript demonstrates light-responsive microposts that can be actuated to perform complex motions, triggered by UV-illumination. The microposts are made by standard micromoulding processes from existing liquid-crystal-based materials that include azobenzene as the light-switch. Key to the nature of the motion is the relative orientation of three non-colinear axes: that of the molecular alignment, that of the geometrical structure (*i.e.* main axis of the microposts), and that of the light direction. Varying these, induces different motions, including non-reciprocal motion. In addition, the manuscript shows that the motion can be steered by varying intensity of the illumination, micropost geometry, temperature, and irradiation intervals/duration.

The manuscript is convincing; results support the conclusions, and methods are well described. Experimental work is combined with numerical computations – the results compare well, and the numerical model has been used both to understand and to direct experiments.

The proposed approach is elegant, simple, and effective – the possibility of achieving different types of motion depending on the relative orientation of the three axes mentioned has not been shown before as far as I know, perhaps because most of the work on these and similar light-responsive materials have been done with thin film structures (for which this will be hard to realize, if not impossible) rather than the 3-D microposts presented here. This makes the approach novel. The manuscript triggers many novel ideas and may be important for future applications in soft robotics, medical applications, and energy materials, and it will be an inspiration for scientists working on light-responsive materials and structures.

My conclusion is that the manuscript can be acceptable for Nature.

Response: We would like to thank the reviewer for their accurate summary and positive assessment of our work and, in particular, for pointing out the differences between our system and the one of traditional thin film structures.

Reviewer comment: I do have some comments / questions to be addressed.

Time constant in experiments: the manuscript mentions a time constant of about 9 s of the azobenzene crosslinker (see supp. Figure 4); however the timescale of the actuation might be different (likely much larger), since this depends on molecular structure (*e.g.* crosslink density), geometry, light intensity, etc. Indeed, a timescale of minutes is mentioned (line 173). What would be the limit here? For speeding this up, could still the same material system be used? This is important for some of the applications mentioned.

Response: The reviewer raises an interesting and salient point. The short answer is that with the same material system but with different azobenzene crosslinkers, the response can be sped up. Azobenzenes with a $t_{1/2}$ in the range of milliseconds are well-known and often used for real-time information transmitting materials (*Beilstein J Org Chem*., **2012**, *8*, 1003–1017) and biological vision restoration (*Angew. Chem. Int. Ed.*, **2011**, *50* (51), 12156-12182). A 2017 study by Broer, Selinger, and co-workers (*Nature*, **2017**, *546*, 632-636; current Ref. 28 in the manuscript) investigated the thermal half-live of azobenzene additives in liquid crystalline polymers for fast undulating movements in thin films. They demonstrate that the performance of the thin films can be influenced by the kinetics of azobenzene switching and relaxation and compare the relaxation behaviors of various azobenzenes within a liquid crystalline polymer matrix. For example, they show that A6MA, which is related to the crosslinker used in this study, has a thermal half-live of > 1000 s at 30 °C, whereas push-pull photoswitches such as Disperse Red (DR1A) have a $t_{1/2}$ < 1 s.

The longer answer is that both for the forward power-stroke and the reverse movement the azobenzene switching dynamics and their coupling to the elastomeric matrix have to be taken into account, as detailed below:

The power-stroke: Photoswitching (= *trans*-to-*cis* isomerization) of the azobenzene is generally very fast (on the timescale of a few nanoseconds, see *Chem. Soc. Rev.*, **2012**, *41* (5), 1809-1825). In a light-driven actuator, the limiting timescale is not the switching of a single molecule, but the much more slowly proceeding (timescale of seconds) bulk isomerization and the traveling isomerization front (Deep optical penetration dynamics in photobending. *Phys. Rev. E*, **2015**, *92* (1), 013206). This bulk photoswitching depends on the switching mechanism, photoswitching quantum yield, molar extinction coefficient, light-intensity, thermal half-life of the reverse reaction, and the concentration of the photoswitch in the sample. Forming a distinct bimorph within the microstructure requires a relatively high concentration of the absorbing species, while propagation of activation through the material requires high light intensity. Dynamic mechanical analysis (DMA) measurements (**Fig. R1**) suggest that within the 60-90 °C temperature range, the azo-LCE is in its rubbery regime and does not show noticeable viscous behavior within the range of 1-100 Hz frequency under a compression strain of 1%. Henceforth, we estimate that the speed of the power-stroke is mainly determined by the bulk-isomerization kinetics of the photoswitch ensembles, which is in the tens of seconds regime, which also fits well with earlier estimations by Warner and co-workers (*Phys. Rev. E*, **2015**, *92* (1), 013206). In our simulation model too, changes in the isomerized fraction are assumed to change the local nematic order parameter, which is in turn coupled to the strain in the free energy computed for each finite element. Both the isomerization and strain free energy are updated at each time step. We note that the photomechanical actuation mechanism in our system is essential for these considerations, as the often-observed photothermal mechanism would lead to different kinetics (*e.g.*, *Adv. Mater.*, **2017**, *29* (18), 1606712). Moreover, one would expect that increasing the crosslinking density of the polymer matrix could slow photoswitching.

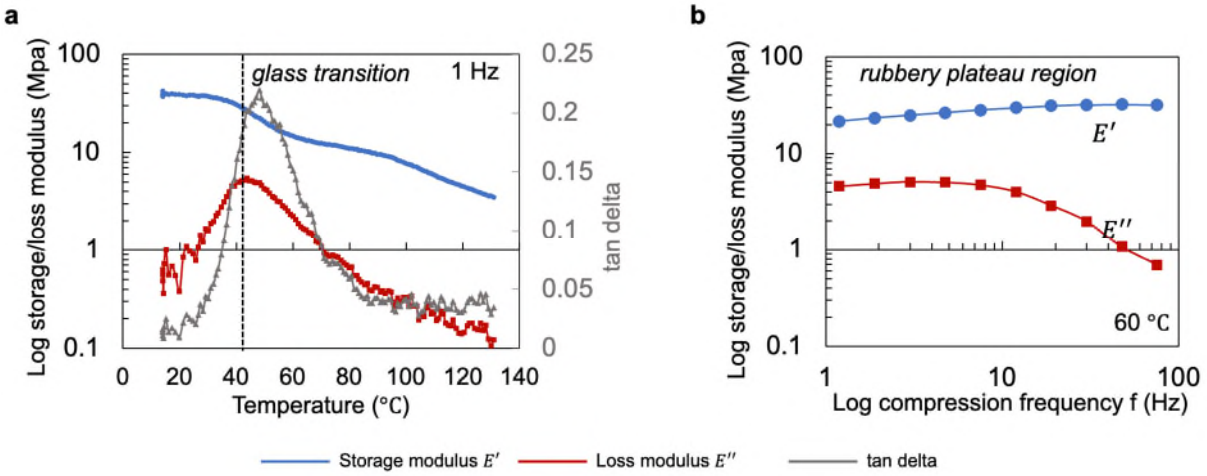

Fig. R1 | Temperature sweep (**a**) and frequency sweep (**b**) dynamic mechanical analysis (DMA) graphs of a bulk azobenzene-LCE disc (thickness 300 µm, diameter 4 mm) under a compression strain of 1%. Data collected on Mettler Toledo DMA 1 dynamic mechanical analyzer under compression mode. A heating rate of 5 °C/min was used for the experiment in (**a**). Both indicate that our LCE is in its rubbery stable under our UV-actuation conditions of 60-100 °C.

Reverse movement: The thermal isomerization from *cis*-to-*trans* heavily depends on the molecular structure and the environment. Thermal half-lives ($t_{1/2}$) can generally be tuned from milliseconds to years. While unfunctionalized azobenzenes generally have a thermal isomerization half-life of above > 8 h, installing two electron-donating groups (push-push) or an electron-donating and an electron-withdrawing group (push-pull) at the respective para positions significantly shortens the thermal half-life (see discussion of aAB and ppAB structures in *Chem. Soc. Rev.*, **2012**, *41* (5), 1809-1825). Polar solvents generally speed up thermal isomerization reactions, as they favor the zwitter-ionic resonance structure with a freely rotatable N-N bond (see scheme 2 in the reference above). As for the power

stroke, we assume that azobenzene switching kinetics are rate-limiting and that (re-)establishing the nematic order together with polymer deformation is comparatively faster, at least for thermal half-lives down to second timescales. To support this, we have conducted new experiments to measure the thermal half-life of the azobenzene crosslinker in the LCE elastomer matrix at 60 °C (temperature is limited by the heating capability of the heat sink) with UV-Vis spectroscopy, which is determined to be $t_{1/2}$~ 40 s (reported here as **Fig. R2** and added to SI as new Supplementary Fig. **S5c** and existing Fig. **S21b**). The result matches well with the $t_{1/2}$~ 34 s calculated from the deformation relaxation of the micropost under optical microscopy at slightly higher temperature (65 °C). As we show in Manuscript **Fig. 3g** and Supplementary Fig. **21**, when increasing the temperature, the micropost exhibits a faster relaxation back to the initial shape with a $t_{1/2}$~ 17 s at 85 °C and $t_{1/2}$~ 6 s at 105 °C. A sped up thermal relaxation, however, will also affect the photothermal stationary states achievable in each activated layer, as the isomerization front propagates, causing the propagating isomerization front to stop earlier as discussed for Manuscript **Fig. 3g**.

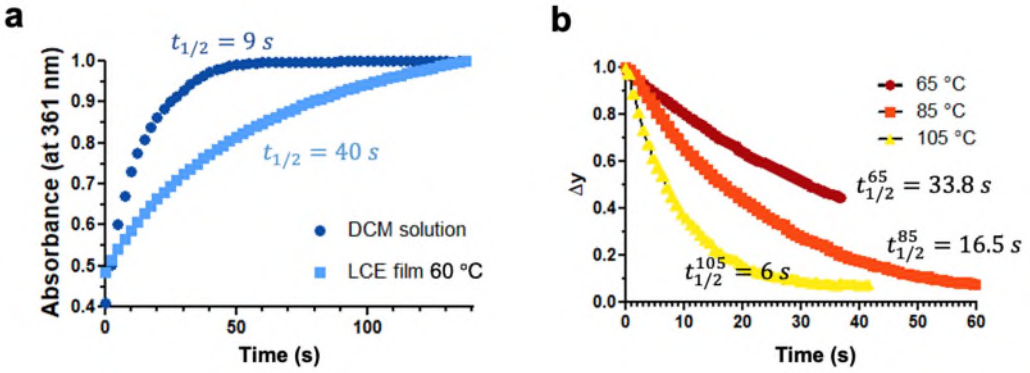

Fig. R2 | (a) Thermal half-lives of azobenzene in solution (dichloromethane) at room temperature and LCE film at 60 °C determined by UV-Vis microscopy (from Supplementary Fig. **5c**), and (b) in an LCE micropost calculated by the relaxation of the y-displacement of the deformed micropost under 65 °C, 85 °C, and 105 °C (from Supplementary Fig. **21b**).

Further control knobs for kinetics of material actuation: There are ample possibilities for tuning material properties with relatively simple means to speed up the power stroke kinetics: one can increase the temperature or change the cross-linking density to increase elasticity of the post. Or one can further increase light-intensity, decrease the diameter of the microposts, or lower the concentration of photoresponsive crosslinkers to speed up the time to bulk isomerization. We already discuss some of these data: **Manuscript Fig. 3g** shows how by increasing the temperature, which also softens the material, we observe increased kinetics and amplitude of the deformation (see also Supplementary Fig. **21**, Video **10**). One could also switch to poly-siloxane-type LCEs, that likely would exhibit faster switching and deformation. Regarding the geometry, there is a lower limit of micropost size that is determined by the unavoidable surface alignment that comes with molding, which we have estimated previously to be of the order of ~5 μm (PNAS, **2018**, *115* (51), 12950-12955). When increasing the light-intensity or decreasing the azobenzene concentration, care has to be taken to still have enough absorption within the micropost to form a transient bimorph. The overall gain in speed will be rather limited and not lie in the orders of magnitude.

With regard to speeding up the thermal relaxation, we are currently pursuing further this avenue by chemically tailoring the azobenzenes for faster thermal relaxation. We envision that actuation frequencies approaching several Hz should be achievable with further optimization. (Indeed, the work by Selinger, Broer, and co-workers cited above, achieves oscillation frequencies of up to 3Hz). However, there will likely be a limit to the highest beating frequency achievable that is significantly less than for high frequency natural cilia (beating in kHz) ("The multiscale physics of cilia and flagella". *Nat. Rev. Phys.*, **2020**, *2* (2), 74-88).

We have added the following sentence to the manuscript page 7/8, lines 272-273:

> *"Note that ample means are readily available for further speeding up the deformation by decreasing the thickness of the micropost, lowering the concentration of the azobenzene crosslinkers, or extending to other photochemistries[33]."*

We further updated manuscript p. 5, lines 170-171:

> *"Once the light is switched off, the post directly returns to its original state, because the cis-isomer of the photoswitchable crosslinker is thermally unstable (e.g. thermal half-life of the cis-isomer[43] was determined to be $t_{1/2}$ = 40 s in the LCE film at 60 °C, Supplementary Fig. **5**)."*

SI page 4, section 1.2.1:

> ***"UV-visible spectra** were obtained on an Agilent 8453 UV-vis diode array spectrophotometer equipped with a peltier-based temperature-controlled cuvette holder. Samples were prepared with Uvasol®-grade solvents and measured in quartz cuvettes of 10 mm pathlength. The obtained UV/vis spectra were baseline corrected. Data-analysis was performed using R (https://www.r-project.org/), GraphPad Prism, or Spectragryph software. Photoswitching of crosslinker **2** in dichloromethane solution was performed with a LED M365F1 (Thorlabs) at room temperature. Spectra for photoswitching within a polymeric thin film (non-aligned LCE, with 7.5 wt% compound **2** as crosslinkers) were collected at 60 °C by immersing the polymer film in quartz cuvettes filled with water upon irradiation with LED M365FP1 (Thorlabs)."*

SI page 7, section 1.2.4:

> ***"Synthesis of the LCE thin film** for UV-Visible measurements: We applied ~10 mg of the reactive monomer mixture onto a flat rectangular PDMS slab on a hot plate at 80 °C (isotropic phase) and placed two 6 µm plastic spacers at the two ends of the PDMS slab. We then covered the molten mixtures with a microscopy glass cover slip (held in place by Kapton®-tape). Cooling and polymerization of the thin film were conducted under the same conditions as for the LCE microstructure described above. After ~1 h of polymerization, the sample was cooled down to room temperature and the PDMS mold and spacers were carefully removed leaving the thin film attached on the cover slip. The cover slip was later cut into a narrow piece to be able to fit into the quartz cuvettes of 10 mm pathlength for the UV-Vis measurements."*

And Supplementary Fig. **5c**, page 16:

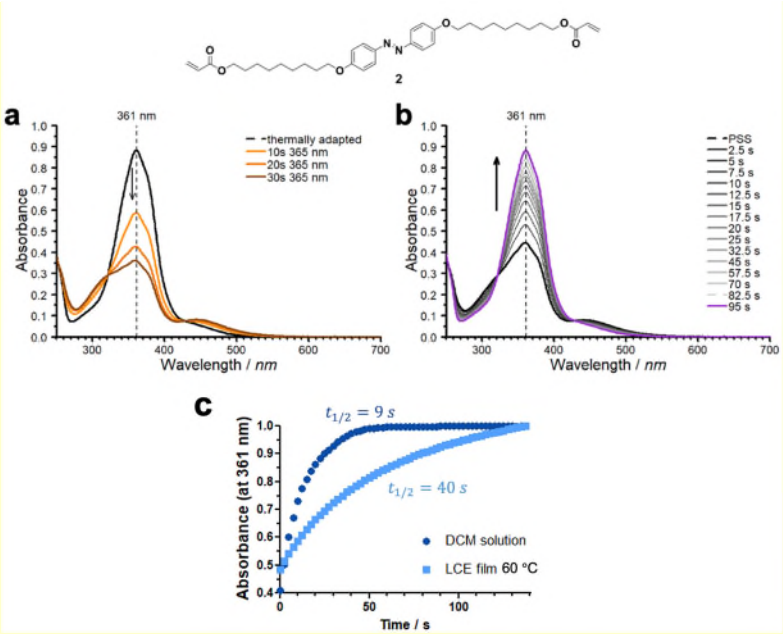

*"**Supplementary Figure 5 |** Representative absorption spectra for the photoisomerization of compound **2** (Synthon Chemicals, ST04181; λ_{max} = 361 nm, in dichloromethane; 293 K): **a.** Photoswitching from trans- to cis-isomer with 365 nm (ThorLabs, LED M365F1), and **b.** Thermal relaxation from cis- to trans-isomer in the dark (PSS = photostationary state). **c.** Determination of thermal half-life of the cis-isomer for compound **2** in dichloromethane (DCM) solution (as shown in part **b**) and in an LCE film under 60 °C: points correspond to measured data (observed at λ_{max}=361 nm). The thermal half-life of the cis-isomer was determined to $t_{1/2}$ ~9 s in dichloromethane solution and $t_{1/2}$ ~40 s in an LCE film at 60 °C. As one can tell from the comparison of the two, the thermal cis-to-trans relaxation rate strongly depends on the local molecular environment; dichloromethane as solvent was chosen for solubility."*

Reviewer comment: Time constant in computations: the SI mentions a relaxation time of 120 s (line 262, SI). How was this determined? Fitting with experiments? It seems, indeed, that the time-dependent behavior is captured well by the model, from Video 6 for example where the experiment and the computation seem to move synchronously. Are we indeed looking at the same timescales for the experiment and the computation here, or has any scaling been done?

Response: The relaxation time was roughly estimated from experimental results, which indicated that the global relaxation of the microstructures should occur on the timescale of minutes. This was sufficient to capture the shape of the experimentally observed trajectories, however the results were rescaled in time for the video.

We've added a note to the caption of **Manuscript Fig. 3a** (page 6, lines 204-205):

*"**Figure 3 | Evolution and high-resolution programming of stroke-like motions. a.** Juxtaposed computationally simulated (top two rows) and experimental data (bottom) capturing the traveling isomerization wave[30,31] resulting from the trans- (blue) to cis- (yellow) photoisomerization of the azobenzene crosslinker, the corresponding complex evolving bimorph, and the ensuing stroke-like deformation of the microstructure at high light intensity (115 mW/cm^2) for out-of-plane irradiation of a micropost with oblique director alignment (ϑ=52°). Simulation results were rescaled in time for the experiment."*

and to Supplementary Video **6** (page 37) to indicate the scaling:

*"**Supplementary Video 6 |** Qualitative agreement of experimentally observed and theoretically predicted (finite-element simulations, SI section 2.1) micropost deformations for*

oblique-aligned microposts irradiated out-of-plane at high- (115 mW/cm^2), medium- (42 mW/cm^2), and low- (15 mW/cm^2) light intensity. Simulation results were rescaled in time for the experiment."

Reviewer comment: Stiffness. The manuscript does not mention an experimental (shear) modulus (but I may have missed it) – is this known? In the computations, a shear modulus of 570kPa has been used (SI, line 242). This is relatively low for a structure that may need to do mechanical work (at least that would be needed for some of the applications mentioned). Do the authors have an idea of the work that can be performed by the actuators? What forces could they apply / resist?

Response: We thank the reviewer for bringing up this important point. For determining the mechanical work that the deforming microstructures can achieve, it is important to note that the ratio of their shear modulus to strain-nematic coupling dictates how much the material will contract along the nematic axis and expand along the orthogonal axes when the nematic order parameter decreases. This ratio was initially (*PNAS*, **2018**, *115* (51), 12950-12955, our work, reference 35 in the current manuscript) fit from experimental results for the simulation model, which was sufficient to predict the light-driven behavior of the system. To better predict the response of microstructures subject to any external loading, we have conducted dynamic mechanical analysis (DMA) on bulk azo-LCEs to experimentally measure the shear modulus of our material, which gives a shear modulus of roughly 4.7 MPa at 65 °C. Based on this result, we estimate the output force of a pillar by the force required to bend a cantilever beam with the same dimension of the pillar. The force can be expressed by $F = 3EI\delta/l^3$, where $I = a^4/12$ is the moment of inertia of the pillar. Therefore $F = Ea^4\delta/4l^3$. Let us consider a pillar with height $l = 150\,\mu m$, edge length $a = 30\,\mu m$ and Young's modulus of $E = 4.7$ MPa, which according to our experiment displaces up to around $\delta = 30\,\mu$m. This pillar thus exerts a force of roughly $F = 8.5\,\mu$N. Compared to its own mass $m = \rho a^2 l = 1.35 \times 10^{-7}$g (assuming that the density of the material is the same as water) subjected to a gravitational force of $F_g = mg = 1.32 \times 10^{-3}\mu$N =1320 pN, the output force then provides a high ratio of $F/F_g = 6439 \approx 6000$. In other words, as a micro-robot, it will have enough power to move around other micro-objects that are 6000 times of its own mass. The output work can be approximated by integrating the force F over the top displacement δ as $\int_0^\delta F(\delta')\,d\delta' \approx 127.5$ pJ, where 1 pJ = 10^{-12}J. Putting this into context, our micropillar has sufficient power to move around micro-objects such as a microparticle of diameter ~1000 μm. What is more, if we are considering biological applications such as dynamic mechanical perturbations of cells in cell culture, the output force ($F = 8.5\,\mu$N) of our microposts is comparable to the contraction force of a single vascular smooth muscle cell (SMC) triggered by Ca^{2+}, which was measured to be $5.7\pm3.1\,\mu$N (Selected contribution: Mechanical strain increases force production and calcium sensitivity in cultured airway smooth muscle cells. *J. Appl. Physiology*, **2000**, *89* (5), 2092-2098).

Reviewer comment: Finally, the actuators indeed can make complex motions. In all examples shown however, these are start-stop motions, that is, the motion is not perpetual unless the light source is switched on and off. Would it be conceivable to design structures with perpetual self-sustained motion (*e.g.* oscillation) under the influence of continuous illumination? The manuscript starts with the example of cilia that show this type of non-reciprocal oscillatory motion.

Response: We thank the reviewer for this very interesting question. As detailed in our response to Reviewer #1's first question, our 3D microactuators are not self-oscillators, either by the design or by the resulting motion. The mechanism of our actuators operating under global directional illumination is fundamentally different from a self-oscillatory system: for the latter, often a carefully positioned local light spot is required and the oscillator switches between two endpoints with unstable intermediate states, whereas the bottom-up feedback within our microactuators under global

uniform illumination enables a succession of controllable and stable deformations along the non-reciprocal motion path. Instead of self-sustained oscillation, what one gains in our system is an almost infinite possible set of programmable deformation trajectories.

Nevertheless, while not the focus of this paper, it is interesting to consider whether—given the design principles of our system—self-sustained motion could be feasible. We provide two scenarios to address this question:

(i) for a single micropillar, we can anticipate that a straightforward approach would be to implement local irradiation (instead of global) in an appropriately flexible system to generate a traditional self-oscillatory system (such as: *Soft Matter*, **2008**, *4*, 1796-1798 or *Soft Matter*, **2010**, *6*, 779-783, among other examples) based on self-shadowing. This motion would likely open other exciting avenues when combined with the dynamic symmetry breakings and self-induced transparency our system offers to go beyond two-state oscillations. Indeed, the effect of topical, site-specific illumination is being one of the directions in our follow-up studies.

(ii) Continuous motion—but not oscillations—can be obtained in our micropost 2D arrays with particularly interesting results: changing patterns of deformations and self-organization can be observed as one varies the direction of illumination over time, reported here in Fig. R3. Because the asymmetric time- and location-dependent self-exposure in different pillars is the foundation of the formation of self-sorted patterns, as long as the azobenzene thermal relaxation kinetics allows for the bimorph re-orientation happening concurrent with changing the light direction, the microarray will switch between different patterns perpetually without the need for turning UV off for resetting the bimorph. Furthermore, as one continues to optimize the sensitivity of the string's response to the light direction or any environmental changes, we envision that "noisy" environmental stimuli and/or built-in noisy responses might be able to enable self-sustained motions—self-sustained reorganization of the self-sorted reconfiguration patterns—in the LCE ensemble system (an approach explored by the Schenning group utilizing the forward and backward isomerization of fluorinated azobenzene and temperature fluctuations under sun light exposure as well as the inhomogeneous softening effect. "A chaotic self-oscillating sunlight-driven polymer actuator". (*Nat. comm.*, **2016** *7* (1), 1-8)

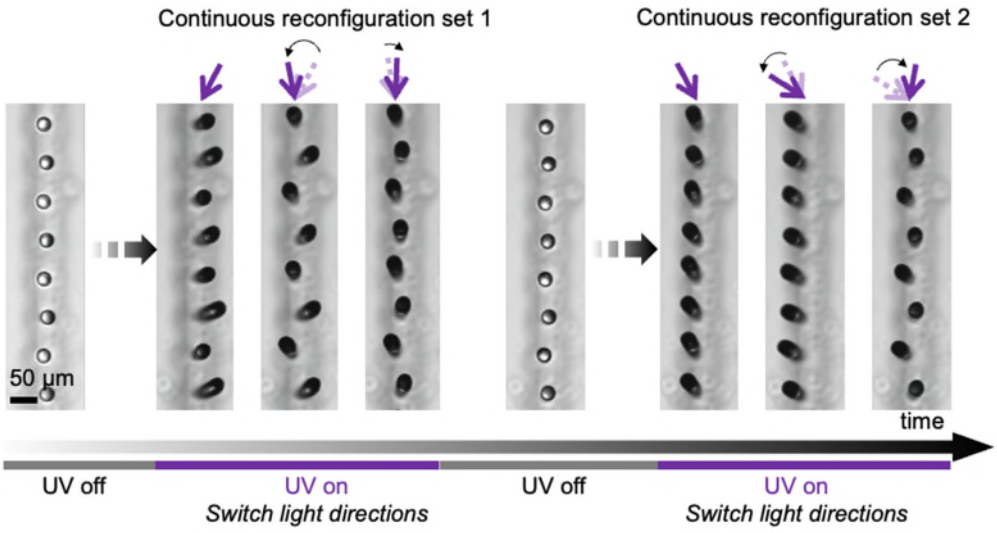

Fig. R3 | Continuous reconfiguration in a string of micropillars when slightly varying the angle of the light source. Note that UV is kept on during the whole actuation period of set 1 and set 2. The orientation of purple arrows is

exaggerated for visualisation purposes. The actual change and deflection from the string axis is around 1-5 degrees.

Referee #4:

Reviewer comment: Novel opto-mechanical cilia actuator which can demonstrate complex motion, as a function of illumination direction and intensity. Interesting methods for fabrication of built-in anisotropy in liquid crystal material in each cilia of the array, which then demonstrates some unique behavior.

These results are exciting and novel development in the field.

Data analysis and methodology are robust and complete.

Response: We thank the reviewer for the positive evaluation.

Reviewer comment: Can the author answer the following questions please.

Page 3, figure 1d, what is the means of magnetic alignment of the molecules in the material?

Response: The liquid crystalline elastomer microposts are molded from a PDMS negative mold as detailed in the SI section 1.2.4 and updated Supplementary Fig. **3**, reproduced below as a response to reviewer. The calamitic (rod-shaped) liquid crystalline monomers are aligned before UV-polymerization in an externally applied magnetic field from commercially available permanent magnets (NdFeB, 1" x 1/2" x 1/2", BX088SH, K&J magnetics, Inc.). By simply changing the orientation of the mold within the magnetic field, any arbitrary uniaxial director direction in 3D can be encrypted into the LCE microstructures. This procedure simplifies fabrication significantly compared to other existing methods including surface alignment or two-step polymerization and mechanical stretching. We note that achieving the oblique molecular (mesogen) orientation with respect to the micropillar principal axis is only accessible through magnetic alignment and cannot be achieved by the existing alignment methods for 3D structures in the 10-100 μm size range. Importantly, after molding and polymerization in directional magnetic field, no magnetic field is further used for the actuation of the pillars!

The alignment of the liquid crystal mesogens has been well-characterized. Mesogens **1** ((4''-acryloyloxybutyl) 2,5-di(4'-butyloxybenzoyloxy)benzoate) are diamagnetic. When placed in a magnetic field, the aromatic units induce a magnetic moment in opposition to the applied magnetic field and thereby raise the free energy of the system. The free energy density in LC mesogens in a magnetic field is captured by the equation below (Demus, Dietrich, John W. Goodby, George W. Gray, Hans W. Spiess, and Volkmar Vill, eds. Handbook of liquid crystals, Volume 2A: Low molecular weight liquid crystals I: calamitic liquid crystals. John Wiley & Sons, 2011):

$$g_{mag} = g_0 - \frac{1}{2}\mu_0^{-1}B^2\chi_\perp - \frac{1}{2}\mu_0^{-1}\Delta\chi(\mathbf{B}\cdot\mathbf{n})^2$$

where $\Delta\chi = \chi_{//} - \chi_\perp$, $\chi_{//}$ and $\chi_\perp$ are the magnetic susceptibilities parallel and perpendicular to the LC mesogens principal axis, respectively. μ_0 denotes the permeability of free space, and **B** refers to the magnetic field and **n** is the director. For most calamitic mesogens, both $\chi_{//}$ and $\chi_\perp$ are negative but the delocalized charge makes a major contribution to $\chi_\perp$ resulting in $|\chi_\perp| > |\chi_{//}|$ and $\Delta\chi$ positive. Therefore, in order to minimize the free energy, the director **n** will align parallel to the magnetic field **B**.

We have added the above discussion to the SI section 1.2.4 and Supplementary Fig. **3b** (page 15) reproduced below (the new portion added to the caption is highlighted in yellow).

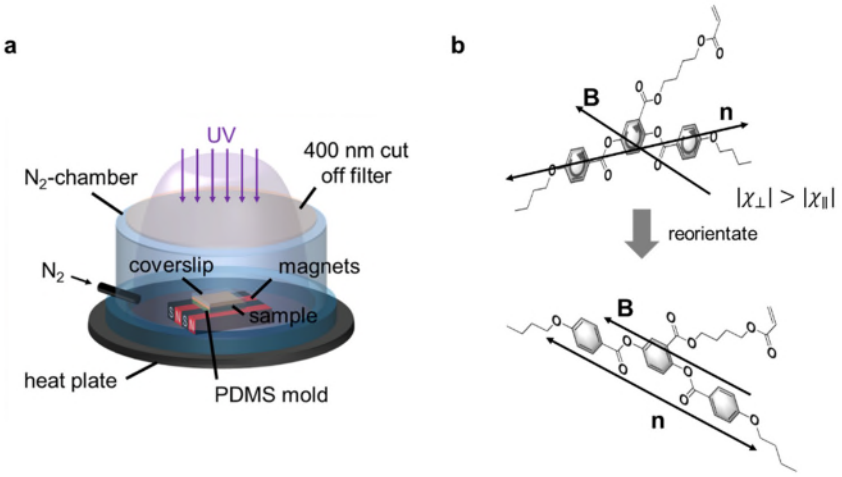

*"**Supplementary Figure 3 | a**. Schematic depiction of the experimental setup for the synthesis of microstructured LCE surfaces: a custom-built inert atmosphere chamber with a 400 nm optical cut-off filter (Newport FSQ-GG400) was placed on a conventional heatplate into a UV-curing chamber (Dymax 2000-EC). Commercially available permanent magnets (~ 0.5 T, K&J Magnetics BX088SH) were placed directly on the heating plate, followed by the PDMS negative mold, the LCE monomer mixture, and a coverslip (all held in place by Kapton®-tape). For more details, please refer to SI section 1.2.4. **b.** Diamagnetism and alignment of calamitic mesogen **1** ((4"-acryloyloxybutyl) 2,5-di(4'-butyloxybenzoyloxy)benzoate) in an applied magnetic field **B**. $\chi_{\parallel}$ and $\chi_{\perp}$ are the magnetic susceptibilities parallel and perpendicular to the LC mesogens principal axis, respectively. **n** denotes the LC director orientation."*

The adapted text in SI section 1.2.4., page 6, now reads:

*"**Comment on the mechanism of magnetic alignment:** The propensity of monomer **1** ((4"-acryloyloxybutyl) 2,5-di(4'-butyloxybenzoyloxy)benzoate), a type of calacmitic LC mesogen, to align within a magnetic field is well-established[3,7,8]. Calamitic LCs are often diamagnetic due to a zero-net spin and the dispersed electron distribution associated with the delocalized charge, for example, from phenyl rings in the mesogen structure. When placed in a magnetic field, the ring currents associated with these aromatic units induce a magnetic moment perpendicular to the conjugated aromatic ring plane in opposition to the applied magnetic field, which thereby raises the free energy. The density of free energy g_{mag} in LC mesogens in a magnetic field can be expressed as[9]:*

$$g_{mag} = g_0 - \frac{1}{2}\mu_0^{-1}B^2\chi_{\perp} - \frac{1}{2}\mu_0^{-1}\Delta\chi(\boldsymbol{B}\cdot\boldsymbol{n})^2$$

*where $\Delta\chi = \chi_{\parallel} - \chi_{\perp}$, with $\chi_{\parallel}$ and $\chi_{\perp}$ being the magnetic susceptibilities parallel and perpendicular to the LC mesogen principal axis, respectively. μ_0 denotes the permeability of free space, and $\boldsymbol{B}$ refers to the magnetic field and $\boldsymbol{n}$ is the director. For most calamitic LCs, both $\chi_{\parallel}$ and $\chi_{\perp}$ are negative but the delocalized electron density makes a major contribution to $\chi_{\perp}$ resulting in $|\chi_{\perp}| > |\chi_{\parallel}|$ and $\Delta\chi$ positive. Therefore, in order to minimize the free energy, the director $\boldsymbol{n}$ will align parallel to the magnetic field $\boldsymbol{B}$[9] (Supplementary Figure **3b**). In our research, we use an externally applied weak magnetic field (~0.5 T) to encrypt molecular anisotropy to our molded LCE microstructures having arbitrary uniaxial director orientation in 3D by simply changing the orientation of the mold within the static magnetic field."*

Reviewer comment: Page 4, lines 122, why was an angle of 45 deg selected for the alignment?

Response: Non-coalignment of the ***MGL*** axes (molecular anisotropy – ***M***, geometrical axis – ***G***, and illumination direction – ***L***) is the basic requirement for multi-modal deformations and, together with a propagating order-to-disorder transition, key to the self-regulation. In principle, any tilted director will give rise to a 'dancing' motion. Initially, we chose a tilt angle of 45°, anticipating the greatest response to the order-to-disorder phase transition at this angle. However, upon closer inspection of the angle effect of the molecular alignment from our finite element simulation model (Model **1**, SI section 2.1, pages 8-9) and mathematical mechanical model (Model **2**, SI section 2.2, pages 10-11), we set the actual angle of our director alignment to be in the range of 50°-60°; this value was obtained by calibrating the experimental values to the simulation results (*see:* Aizenberg, *et al* "Multiresponsive polymeric microstructures with encoded predetermined and self-regulated deformability". *PNAS*, **2018** *115* (51), 12950-12955). The simulation results shown in **Manuscript Fig. 3a** illustrate the case for a micropost with molecular alignment of 52° degree.

We have adjusted the main text of the manuscript to avoid confusion and to be consistent with the later discussion in **Manuscript Fig. 3e** on the influence of steepness of the director alignment. We also added a note to specify the angle used in simulation to the figure caption of **Manuscript Fig. 3a**.

The adjusted manuscript text now reads, page 3, lines 118-121:

> *"To program molecular anisotropy oblique to the structure's principal axis, we first chose a director orientation of around the midpoint of 0° and 90° with respect to the Z-axis of the square micropost in the YZ-plane (indicated by the blue double arrow in **Fig. 1e**) as one would expect here the most pronounced tilting deformation upon bulk order-to-disorder phase transition."*

As well as **Manuscript Fig. 3**, legend, page 6, lines 204-295:

> *"**Fig. 3a.** Juxtaposed computationally simulated (top two rows) and experimental data (bottom) capturing the traveling isomerization wave[30,31] resulting from the trans- (blue) to cis- (yellow) photoisomerization of the azobenzene crosslinker, the corresponding complex evolving bimorph, and the ensuing stroke-like deformation of the microstructure at high light intensity (115 mW/cm^2) for out-of-plane irradiation of a micropost with oblique director alignment (ϑ=52°). Simulation results were rescaled in time for the experiment."*

Regarding the angle effect, we describe in **Manuscript Fig. 3e** for two cases of $\vartheta \geq 60°$ and $\vartheta \leq 45°$, (see also Supplementary Figs. **15**-**19** and mechanical Model **2**), the expansion/contraction of the vertical and horizontal components of the activated layer. These changes in volume drive the post to bend 'away from light' to 'towards the light', as the angle is increased from $\vartheta \leq 45°$ to above $\vartheta \geq 60°$. An initial simulation model by our group (Balazs *et al.*, "Twist again: Dynamically and reversibly controllable chirality in liquid crystalline elastomer microposts." *Sci. Adv.*, **2020**, *6* (13), aay5349) illustrates this concept and shows that the above switch in the orientation of the post happens roughly in between 45°-60°. **Manuscript Fig. 2** has an experimental ϑ of roughly 55°.

We have now added this number to the caption of Manuscript Fig. 2, page 4, line 175.

> *"Confocal laser scanning and scanning electron microscopy (SEM) images of actuated photoresponsive LCE microposts with oblique director alignment of ϑ~55° (tilted with respect to the principal axis into the YZ-plane) upon UV-irradiation (15 mW/cm^2) at their four facets (i. 'back', ii. 'right', iii. 'left', and iv. 'front')."*

Reviewer comment: Page 4, lines 132, is the effect on absorption a photo-bleaching effect, please clarify, this change in absorption characteristics.

Response: We apologize if the phrasing was ambiguous. For the *trans*-to-*cis* photoisomerization—and thus the order-to-disorder transition—to propagate deeper into the LCE, the light absorption of the

material at the wavelength of irradiation (365 nm) needs to decrease significantly. We refer to the latter process as an increase in transparency. As the reviewer points out correctly, such a local drop in absorption could be a result of photodegradation (= decomposition of the photoresponsive species) or photoswitching. The former is an irreversible process, which would only allow a single deformation process and no thermal relaxation, whereas the latter is a reversible process—referred to as a **saturated absorption** (see Warner and co-workers, *Physical Review E*, **2015**, *92* (1), 013206)—which enables repeatable switching. *We have strong evidence that supports a fully reversible process*. Updated Supplementary Fig. **24** shows the robustness of the actuation response >100 cycles with no appreciable fatigue. In addition, the fact that a change in irradiation direction, (see **Manuscript Fig. 3c & e**) and changes in irradiation sequence (periods of ´on´ and ´off´; see **Manuscript Fig. 3h**, Supplementary Figs. **22** & **23**, and Video **12**), allows us to precisely tune the type and trajectory of a single deforming micropillar upon multiple irradiations, rules out a fully photodegradation-based mechanism. Realistically, there will be some photodegradation over very long periods of irradiation, together with other effects of mechanical or chemical aging, which may affect material performance, as is typically observed for any material (´wear-and-tear´). The fact that >100 consecutive cycles are possible without noticeable irreversible aging, however, suggests that such effects are insignificant under the conditions studied.

The updated Supplementary Fig. **24** with updated caption, SI page 30, is reproduced below:

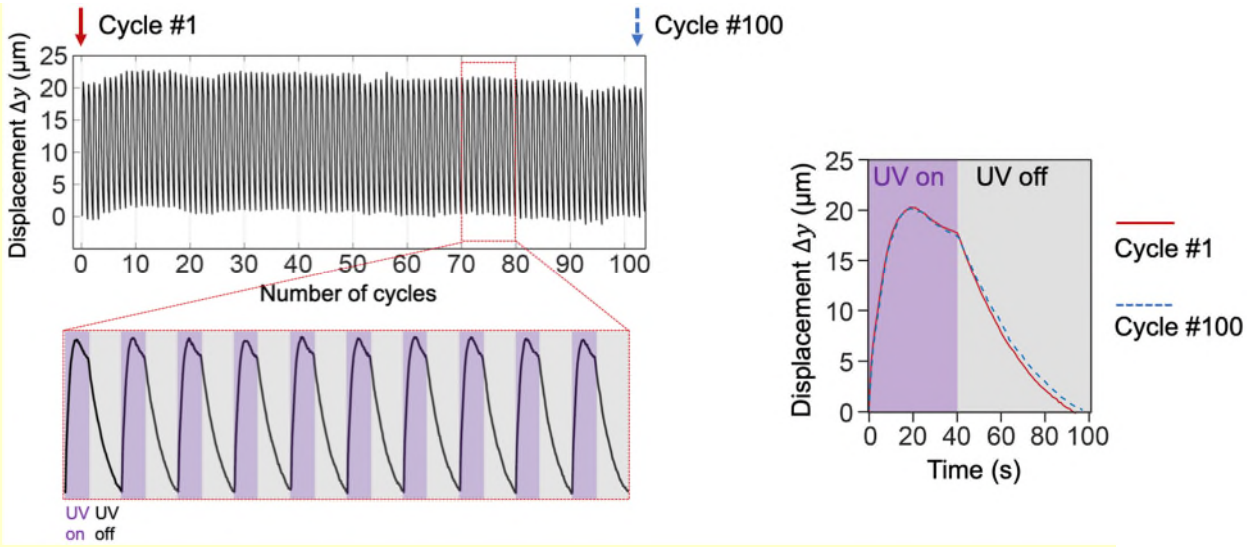

*"**Supplementary Figure 24 |** No considerable fatigue is observed over at least 100 consecutive cycles of photoactuation at 115 mW/cm² for the example of out-of-plane 'dancing' behavior with UV 'on' 40 s and UV 'off' 60 s in each cycle at 60 °C. These results suggest that photodegradation effect is insignificant under the conditions studied."*

We have also slightly expanded SI section 1.2.1 on the process of acquiring these repeated actuations (SI page 4).

***"For UV-irradiations**, an LED mounted in a heatsink (Thorlabs, M365F1) was used and controlled with a T-cube driver (Thorlabs, LEDD1B) for continuous adjustment of light-intensity. Twelve levels of intensity were used: (1) 1.0 mW/cm², (2) 2.5 mW/cm², (3) 4.8 mW/cm², (4) 9.0 mW/cm², (5) 12.6 mW/cm², (6) 15.8 mW/cm², (7) 24.8 mW/cm², (8) 42.1 mW/cm², (9) 66.2 mW/cm², (10) 90 mW/cm², (11) 103.8 mW/cm², and (12) 115.0 mW/cm². Irradiance levels were determined at 1 cm distance from the light-source with a power meter (Thorlabs, S310C in conjunction with PM100D). For irradiation in intervals, a TTL signal provided by an*

Arduino Uno controller was used to switch on or off the LED through the Trigger Mode of the T-cube driver."

Reviewer comment: Page 5, lines 168, when the UV light turns off, does the reaction continue due to diffusion of molecules which are photo-activated within the polymer?

Response: For the purpose of this work, we assume no diffusion of molecules, since all molecules are polymerized into the crosslinked polymer network. Please note that the photoresponsive azobenzene molecule **2** is added as a crosslinker, which we assume to be covalently anchored within the network. To make the polymer, we combine 90.5 mg side-chain mesogen **1**, 7.5 mg of the azobenzene crosslinker, and 2 mg of Irgacure 819 as photoinitiator. This amounts to a 8 mol% crosslinking density. The polymer (microscale thickness ~ 150μm) undergoes free radical polymerization for 1h (see SI section 1.2.4 & 1.2.5). We cannot rule out any unpolymerized species, but given the fabrication conditions, it is unlikely that significant amounts of unpolymerized monomers/crosslinkers are still present in the material. This is supported by the fact that repeated thermal cycling above the T_{NI} of the material does not lead to melting, which would be expected for incomplete polymerization.

Another factor speaks against diffusion of photoactivated molecules: a photomechanical mechanism of actuation: Monitoring the micropost deformation with an IR camera, we observe no significant photothermal heating (see Supplementary Fig. **6**, Video **1**, SI section 1.2.1). Similarly, immersion of the microposts into water, which should efficiently suppress any photothermal mechanism, shows normal photoactuation behavior (see Supplementary Fig. **7**). All this experimental evidence strongly supports a photomechanical and not photothermal actuation mechanism, which is often observed. This matters because a photomechanical mechanism relies on the anchoring of the photoresponsive species within the network. Moreover, the absence of significant heating works against potential diffusion of possible negligible amounts of unattached species.

Speaking of a liquid crystal polymer (LCP) system with doped low-molecular-weight azobenzene derivatives, Ikeda reported previously on how the *trans*-to-*cis* isomerization of azobenzene could lead to a phase transition within the LCP (*J. Mater. Chem.,*1 **2003**, *3*, 2037–2057 and *Chem. Lett.*, **1998**, *17*, 1679–1682). However, as pointed out by Qin L. and Yu Y. in *Responsive Polymer Surfaces: Dynamics in Surface Topography* (Liu, Danqing, and Dirk J. Broer, eds. John Wiley & Sons, **2017**, Chapter 1.2), this problem can be addressed by covalently binding the azobenzene moiety to the host polymer matrix. This is the case in our materials.

Reviewer comment: Page 6, line 206, with these high light intensities of 115mW/cm2 after actuation by light, is there any hysteresis present? For example, from thermal expansion of the layers due to heat input from the light absorption?

Response: As mentioned above, the presented material system likely operates under a photomechanical mechanism. No photothermal heating is observed upon actuation of pillars when observed with an IR camera (see Supplementary Fig. **6**, Video **1**, and SI section 1.2.1). Moreover, immersion into water, which should efficiently suppress any thermal actuation pathways, does not impede photoactuation dynamics (see Supplementary Fig. **7**, Video **11**). As is evident from the newly added figure part in Supplementary Fig. **24**, added here as **Fig. R4**, overlay of the 1st and 100th cycle of irradiation (data taken from Supplementary Fig. 24), shows that little to no hysteresis is observed.

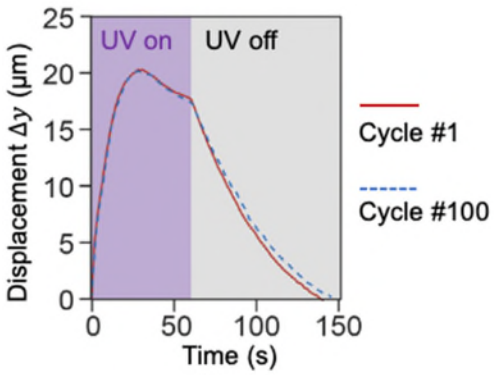

Fig. R4 | Superstacked trajectories of the 1st cycle (red solid line) and the 100th cycle (blue dashed line) of actuation and thermal relaxation for UV-on 40 s and UV-off 70 s. No obvious fatigue of the deformation was observed.

Reviewer comment: Page 7, lines 269, is there an optimum range of temperature for operation of the asymmetric motion of the cilia?

Response: The glass transition temperature of the LCE (T_g) is ~45 °C and the nematic-to-isotropic phase transition temperature (T_{NI}) occurs at ~92 °C (see DSC spectra in Supplementary Figure **4**). Below the glass-transition temperature, actuation is hindered; we made use of this behavior for ´freezing´ the microposts in the deformed state (see **Manuscript Fig. 2**, SEM insets and Supplementary Fig. **11**). As temperature increases, the LCE material will soften, making larger actuation motions possible. In addition, the rate of thermal back-isomerization (*cis*-to-*trans*) of the azobenzene crosslinker increases with increasing temperature, ultimately lowering the achievable photothermal stationary states and thereby reducing penetration depths into the pillar. This is nicely illustrated by **Manuscript Fig. 3g** showing that increasing the temperature yields larger out-of-plane deformation amplitudes and incomplete bulk isomerization. The latter factors change the final deformation position. We make use of this effect for the stable deformation patterns in the **new Manuscript Fig. 4** (reproduced above in its entirety). Taking these two extremes into account, we find experimentally the temperature range of 60-90 °C to be optimal for actuation. This range represents a good compromise between mechanical stiffness and azobenzene back-isomerization kinetics.

We note that all these parameters (T_g and T_{NI} of the material and $t_{1/2}$ of the azobenzene) can easily be tuned by chemical modification. The general principles laid out in the present manuscript, together with the theoretical model, will allow the design of actuators that operate at very different optimal temperature ranges.

Reviewer comment: Page 8, line 305, do these wave like motions have anything in common with cilia motion in clams and oysters?

Response: An interesting point of the cilia-lining on the gills in clams is not just the fact that the metachronal waves in these cilial carpets cause a flow of the surrounding liquid through the siphon, but also that this flow can be regulated through cilial motion and intercilial coordination. Directional flow necessitates non-reciprocal motion of each cilium and collective wave-like patterns. While the non-reciprocal motion is also a feature of our microstructures, the dynamics in these arrays arise from a distinct mechanism. In cases where ***G***, ***L***, & ***M*** are non-coaligned (**new Manuscript Fig. 4e**), the non-reciprocal deformation trajectories of each post within an array influence each other and self-organize into complex patterns of movement. In addition, as our added experimental and theoretical results demonstrate (see discussions above), dynamic changes in temperature, light direction, intensity and irradiation intervals allow us to program many different movement patterns within the same actuator

‘carpet’. The richness of the array patterns has direct consequences for applications from information encryption and information processing to transport and soft robotics.

Reviewer Reports on the First Revision:

Referees' comments:

Referee #1 (Remarks to the Author):

The revision and the response letter have sufficiently addressed my questions and concerns. I, therefore, recommend to accept the paper for publication.

Referee #4 (Remarks to the Author):

Many thanks for the much improved revised manuscript.